



Natural Resources
Canada

Ressources naturelles
Canada

**GEOLOGICAL SURVEY OF CANADA
OPEN FILE 7994**

**Baseline Assessment of Seismic Hazards in British Columbia's
North Coast**

C. Brillon

2016

Canada 



**GEOLOGICAL SURVEY OF CANADA
OPEN FILE 7994**

**Baseline Assessment of Seismic Hazards in British Columbia's
North Coast**

C. Brillon

2016

© Her Majesty the Queen in Right of Canada, as represented by the Minister of Natural Resources Canada, 2016

doi:10.4095/297566

This publication is available for free download through GEOSCAN (<http://geoscan.nrcan.gc.ca/>).

Recommended citation

Brillon, C., 2016. Baseline Assessment of Seismic Hazards in British Columbia's North Coast; Geological Survey of Canada, Open File 7994, 36 p. doi:10.4095/297566

Publications in this series have not been edited; they are released as submitted by the author.

Abstract

A review of existing geohazard studies pertaining to British Columbia's north coast (BCNC), an area with a number of proposed infrastructure projects, revealed that there are many unknowns and scientific gaps with regards to natural geologic hazards in the BCNC. Of particular interest is the potential of earthquakes and slope failures (i.e. landslides) and the relationship between the two. In addition to the well-known 1974 and 1975 Kitimat Arm landslides (Murty, 1979; Murty and Brown, 1979; Conway et al., 2012), recent bathymetric mapping of the Douglas Channel revealed two large submarine landslides and a previously unmapped geomorphic feature that is consistent with active faulting (Conway et al., 2012). Whilst not conclusive, the proximity of the feature to the landslides suggests that movement on the identified fault as a potential landslide trigger.

Historically, the BCNC has been seismically quiescent. As a consequence, seismic monitoring and research related to the BCNC has been minimal. While larger earthquakes are felt and recorded, the configuration of the Canadian National Seismograph Network prior to 2014 did not allow earthquakes less than approximately M_L 2.1 to be consistently located. Long-term, continuous monitoring of microseismicity, combined with geodetic and paleoseismic techniques could be used to assess the possibility of large earthquakes on the recently mapped Douglas Channel "fault". Moreover, these studies could identify other potentially unmapped faults in the BCNC region and provide an indication of their potential to host large earthquakes. Modelling of earthquakes similar to the 1973 M_L 4.9 Terrace earthquake, a hypothetical rupture on the Douglas Channel fault, and a M_W 8.0 Haida Gwaii thrust earthquake reveal that shaking intensities from such earthquakes could be sufficient to induce slope failures in the BCNC.

Regional GPS studies have shown that west and south of the BCNC there is significant crustal deformation (Hippchen, 2011; Mazzotti, et al., 2003a&b). Presently, the hypothesis is that some of the neighbouring deformation and hence strain is being transferred to the BCNC. Augmenting the permanent GPS network will help quantify how much strain is being transferred from surrounding regions to the BCNC, which will subsequently improve seismic hazard knowledge in the region.

This report compiles the state of knowledge of geohazards in the BCNC region prior to 2014. Knowledge gaps are identified and recommendations to minimize those gaps are made. Recent efforts to fill the knowledge gaps are discussed.

Introduction

With a growing number of on-going and planned infrastructure projects, BC's north coast is emerging as a region of high strategic importance to Canada's economy. Consequently, the environment and therefore the economy are vulnerable to the negative impacts of geohazards (and their secondary effects), such as earthquakes and slope failures. Within the Coast Mountains between Prince Rupert and Bella Bella, herein referred to as BCNC (Figure 1), there has been minimal research to understand local earthquake hazards. A more detailed understanding of where and how regional strain energy is being accumulated in the crust and the likelihood of damaging earthquakes in this area is necessary to improve ground shaking hazard models for use in the National Building Code of Canada (e.g. NBCC, 2010). The purpose of this study was to collect existing data to provide a baseline for seismic and GPS studies for the BCNC. This information was used to evaluate potential ground shaking levels and existing relationships between shaking and the triggering of secondary hazards such as landslides (both subaerial and submarine), liquefaction, and tsunami inundation. Moreover, this study was used to determine the optimum targets for seismic and GPS deployments in the BCNC.

Motivation for this study was triggered by the findings from Conway et al. (2012), in which re-analysis of multibeam and bathymetry data retrieved between 2007-2009 revealed evidence that two large (more than 30 km³) submarine slides occurred during the mid-Holocene (Figure 1). The cause of these two failures is unknown; however their proximity to a nearby unmapped fault-like structure (Figure 1) suggests that the slides could have been triggered by strong ground shaking from rupture along this structure (Conway et al., 2012). In addition to these newly discovered slides, two well-known landslides occurred in the 1970's in Kitimat Arm (Figure 1). Both of these recorded slides occurred during low tide, significantly decreasing the impact of the generated tsunamis (Murty, 1979; Murty and Brown, 1979; Conway et al., 2012). On October 17, 1974 a submarine slide generated a 2.8 m tsunami (Murty, 1979). The following year on April 27, 1975, a slope failure on the northeast side of Kitimat Arm (which overlapped the 1974 failure area) displaced an estimated upper limit of 26,000,000 m³ of material (Murty, 1979; Murty and Brown, 1979; Conway, 2013). Watermark observations in Kitimaat Village estimated that the tsunami generated by this slide was up to 8.2 m high. While the trigger of the first event is unknown, the latter event coincided with nearby construction at that time (Campbell and Skermer, 1975). Modelling of the 1975 slide estimates that the generated tsunami waves could have been as high as 11 m (Skvortsov and Bornhold, 2007). Numerous landslides have also been mapped by the BC Department of Forestry in an attempt to improve safety measures for forestry workers (Geertsema et al., 2005; Jakob et al., 2006). The culmination of these studies brings awareness to the significant natural hazards present in the fragile coastal environment of the Coast Ranges.

Climate

The BCNC exists within the Coast Mountains of the Coastal Gap Ecoregion (BC Ministry of Environment). Granitic mountains with rugged, steep slopes dissected by an intricate fjord system dominate this region. While the western coastline is dotted with islands of lower elevation, more inland the Kitimat Range consists of eroded, dome shaped mountains dissected by deep fjords. At lower elevations the land is covered by wet, coastal hemlock forests, whereas higher elevations are characterized by barren rock or mountain hemlock subalpine (BC Ministry of Environment). Moist Pacific air flows across the region bringing intense precipitation to windward slopes and the inland mountains, while cold Arctic air migrates to the area resulting in low temperatures and significant snow levels (BC Ministry of Environment). Temperatures in the region range between -5.5°C in the winter, up to 22°C in the summer. Mean annual precipitation in this region is approximately 2,928 mm/year, with 80-96% of this in the form of rain. On the western most islands average, annual snowfall has been as little as 125 cm, while in Kitimat annual snowfall is often greater than 400 cm (Environment Canada). At higher elevations snow pack is ~140 cm (Schwab, 2011).

Geology

British Columbia (BC) resides within the Canadian Cordillera, which is divided into five distinct margin parallel orogenic belts – the Insular, Coast, Intermontane, Omnicrystalline, and Foreland Belts (Monger et al., 1982; Figure 2). The BCNC lies predominantly within the steep mountain ranges of the Coast Belt, which marks the transition between the Insular and Intermontane Belts (Chardon et al., 1999) and is composed of the Coast Mountain Batholith, the Banks Island Assemblage, the Yukon-Tanana and Alexander terranes and the Gravina Belt (Figure 2, Nelson et al., 2012). The Coast Mountain Batholith is composed mostly of tonolite and granodiorite with smaller amounts of other igneous rocks intruded between 160-50Ma. The Alexander terrane consists of volcanic, sedimentary, and plutonic rocks and their metamorphosed counterparts of late Proterozoic to early Paleozoic age. The Banks assemblage, accumulated during the mid-Paleozoic, is exposed most on Banks and Porcher Islands, but is also interspersed throughout the southern Coast Belt as far south as Klemtu. The Banks Island assemblage is recognized by strongly deformed and metamorphosed interlayered quartzites and marbles and the presence of detrital zircons. The Yukon-Tanana terrane, formed of meta-volcanic and meta-sedimentary rocks, underlies the western portion of the Coast Mountains. Overlaying the Alexander and Yukon-Tanana terranes is the upper-Jurassic to upper-Cretaceous aged turbidites and mafic volcanic rocks of the Gravina belt. For more details of the regional bedrock geology see Gehrels (2009) and Nelson et al. (2012).

During the formation of the western continental margin plutonic belts were accreted to the margin, some of which are marked by N-NW trending coast parallel shear zones. The Coast Mountain shear zone marks the boundary between two magmatic arcs of significantly different ages (105-90 Ma to the west and 80-50 Ma to the east) (Figure 2, Crawford et al., 2005). Other major faults that are preserved within the waterways include the Principe-Laredo, Kitkatla, and Grenville faults (Figure 2). In addition there are two dextral shear zones in the southern part of the BCNC that converge with the Grenville fault (Chardon et al., 1999). At least some of these faults were active during the development of the area since the Miocene (Rohr and Dietrich, 1992).

Following the accretion and intrusion of the major terranes to the West Coast, a period of wide-spread glaciation occurred. During the Pleistocene the Cordilleran ice sheet covered most of BC (Booth et al., 2003). Melt waters from the glacier built a fan-delta of sand and gravel in the sea with finer marine sediments settling further out in the low-energy marine environment (Schwab, 2011). As glaciers retreated to the highest elevations of the Coast Mountains, networks of deep valleys, thickly lined with a rich array of mud, sand, deltaic gravel and till were left behind (Bornhold, 1983, Clague, 1985). The deglaciation of the BCNC is similar to that which occurred along the entire North American coast. However, due to large quantities of sediment transport and periods of stagnation, the thickness of the sediments deposited in the BCNC is much greater (Clague, 1984). In some places, such as Kitimat, glacial moraine is hundreds of metres thick (Bornhold, 1983; Clague, 1984). Following deglaciation the land remained depressed, sea level rose and glaciomarine sediments (clay, silt up to 60-metres-thick) were deposited until the sea level subsided to present-day levels (Bornhold, 1983; Schwab, 2011). As these marine deposits were exposed to fresh water, salts were leached out resulting in saturated, porous sediments (i.e. clay) which are prone to failure (Schwab, 2011). Boreholes in the area have recorded bedrock at depths ranging between 17-106 m (Dolmage, V., 1956).

Tectonics

The west coast of BC encompasses three significant tectonic regimes which contribute to the continuous deformation and seismic hazard surrounding the relatively seismically quiescent BCNC. The predominate tectonic influences are from the northwestward motion of the Pacific plate (PA) relative to the North American plate (NA) and the convergence of the Juan de Fuca (JdF) and NA plates (Figure 1).

North of the BCNC, near the Gulf of Alaska, lays a region of high seismicity due to the relative northward motion of the PA plate with the NA plate (Figure 1). Seismicity in this area decreases to the north, and consists of predominately shallow earthquakes up to M 7.4 which are distributed along secondary faults related to the collision of the Yukutat Terrane (which moves with the PA plate) and North America (Page, et al. 1991).

Directly west of the BCNC lies Haida Gwaii, which has experienced four nearby earthquakes greater than M_w 7.0: 1929, 1949, 1970, 2012 (Figure 1; Rogers 1986; Cassidy et al., 2014; James, et al. 2013). The M_w 8.1 1949 earthquake occurred on the Queen Charlotte Fault (QCF) and is the largest recorded Canadian earthquake (Bostwick, 1984; Lamontagne et al., 2008; Cassidy et al., 2014). The most recent of these events is the October 28, 2012 M_w 7.8 earthquake. This event occurred on a shallow-dipping thrust fault that partitions compressional strain from the steeply dipping strike-slip QCF (James et al., 2013, 2015). The 2012 earthquake was felt as far as the Yukon Territories and Alberta in Canada, and Washington and Montana in the USA. The earthquake was accompanied by a tsunami with run-ups exceeding 3 m (James et al., 2013, 2015; Leonard and Bednarski, 2015).

South of the BCNC is the Cascadia Subduction Zone (CSZ), a result of the convergence of the JdF plate with the NA plate (Figure 1). The lack of seismicity on the plate interface, together with crustal deformation measured by GPS show that the CSZ is currently locked and accumulating strain (Hyndman, 2013 and references therein). Specifically, no mega-thrust earthquakes have been instrumentally recorded on this margin. However, Japanese written records and oral records of the First Nations people on Vancouver Island recount that on January 26, 1700 there was strong shaking followed by a tsunami with wave heights of 2-3 m (recorded in Japan). Modelling of the observed wave heights suggests that a M_w 9.0 earthquake originating near Vancouver Island, BC most likely produced these waves (Satake, et al. 1996, Hyndman et al. 1996). In addition, paleoseismic studies along the west coast of Vancouver Island, Washington and Oregon revealed that 19 similar mega-thrust earthquakes have impacted North America's West Coast in the past 10,000 years (Goldfinger et al., 2012). Due to the ongoing compression of the North American (NA) plate as subduction proceeds numerous crustal earthquakes occur in southwest BC. Likewise, earthquakes are also generated within the JdF plate as it subducts and encounters increasing temperatures and pressures (Ristau et al., 2007).

Existing Knowledge

Seismicity and Seismic Monitoring

Compared to the seismicity north, south and west of the BCNC, the quantity and magnitude of archived earthquakes is significantly less (Figure 3). The absence of significant earthquakes in the BCNC has resulted in a deficiency of permanent instrumentation and research in the area. The paucity of seismic instrumentation leads to knowledge gaps negatively affecting the Seismic Hazard Map of Canada (e.g. Adams and Halchuk, 2003), which underpins earthquake seismic provisions in the National Building Code of Canada (NBCC, 2010).

Between 1971 and 2013, approximately 400 earthquakes (Figures 1&4) have been located in the BCNC by seismologists at Natural Resources Canada (NRCan). The southern border of the BCNC is composed of the Anahim Volcanic Belt (Figures 1&4). Two significant swarms related to this volcanic region (September 1942-August 1943 and October 2007-December 2007) have been observed (Cassidy et al., 2011; Figure 3). On the east side of the BCNC there is a small cluster of events that likely all represent blasting at nearby mines and gravel pits (Figure 4). Offshore, west of the BCNC, numerous events are located within Hecate Strait as well as onshore and offshore Haida Gwaii (Figure 3&4). Aside from these mentioned sources of seismicity, earthquakes are infrequent in the BCNC. There was a small, unfelt swarm (M_L 1.7-2.0) September 13-14, 2010 located near Gil Island (Figure 4). Over the years some earthquakes have also been

located near the recently mapped fault-like structure and the Grenville Channel Fault (Figure 4). However, average errors associated with these events in this specific area are 3.5 km in the east-west direction and 4.9 km in the north-south direction. The largest event that has been recorded in the BCNC is a M_L 4.9 approximately 20 km southwest of Terrace on November 5, 1973 (Figure 4). This event was felt as far as 120 km away, with some minor damage (broken windows and cracked plaster) reported near the epicentre. The maximum intensity reported was V on the Modified Mercalli Intensity (MMI) scale. The main shock was preceded by a M_L 2.5 foreshock 4 hours before, and followed by a felt M_L 3.7 (MMI=III) the day after (Rogers 1976).

Prior to 1951 all earthquake locations in Western Canada were derived from international catalogues that incorporated arrivals of earthquakes recorded on a seismograph in Victoria, BC and/or felt reports (Milne et al., 1978). At that time the completion magnitude in the BCNC was M_L 6.8 (Adams and Halchuck, 2003). By 1951 the first three stations (Victoria, Port Alberni, and Horseshoe Bay) of the Canadian National Seismograph Network (CNSN) had been established in BC, allowing Canada to independently locate large earthquakes in BC. With arrivals from these three stations as well as some USA stations, independent processing of small, local earthquakes in western Canada (Milne et al., 1978) was possible. In 1962 a seismograph was installed in Port Hardy (PHC), on the northern tip of Vancouver Island (Figure 1&3), which was followed in 1965 by the installation of a seismograph in Fort St. James (FSJ) on the BC mainland (Figure 3). The addition of these two stations improved seismic locations in the BCNC and decreased the magnitude completeness (M_C) to M_L 3.8 (Adams and Halchuck 2003). However, it was not until 1971 when a seismograph was installed in Queen Charlotte City (near the current station, MOBC) that there was sufficient station coverage to enable analysts to locate earthquakes in the BCNC as small as M_L 3.3 (Adams and Halchuck 2003). Today, many of these original stations have been moved to nearby locations as shown in Figure 3.

Since 1972 the CNSN has expanded to include seismographs in Bella Bella (BBB), Prince Rupert (RUBB), Bonilla Island (BNAB)(Figure 3). With the addition of these seismographs, the accuracy of earthquake locations in the BCNC significantly improved and the M_C decreased to approximately 2.1. However, with only these permanent CNSN stations, the M_C in the BCNC is still considerably higher than neighbouring regions. Although earthquakes smaller than M_L 2.1 can sometimes be located, the CNSN seismic data is not consistently monitored for such small events and therefore does not guarantee that earthquakes smaller than M_L 2.1 are always identified and located. This has potentially translated to the seismicity gap observed in the BCNC.

In addition to decreasing the M_C , increased station coverage would decrease location uncertainties and allow for improved depth estimation. Prior to 1951 location errors were on the order of ± 100 km adjacent to and including Haida Gwaii and ± 20 km in southern BC (Milne et al., 1978). Current routine earthquake locations in the BCNC use arrivals from permanent CNSN stations as near as 25 km and as far away as 275 km. Most M_L 1-2 events are located with arrivals from only RUBB, BBB, and BNAB. M_L 2-3 events include additional arrivals from stations on Haida Gwaii and sometimes BNB, FSB and UBRB, while M_L 3+ events always use arrivals from these additional stations. For events within the BCNC from 1992-2014 average, calculated errors are ~ 7 km in the north-south direction and ~ 4 km in the east-west direction. Errors in the north-south direction are usually due to the absence of stations and therefore arrivals north and south of the BCNC, while errors in the east-west direction are attributed to the bias of stations west of the BCNC (Haida Gwaii). These errors represent the minimum location errors. Random (i.e. picking) and systematic (i.e. generalized velocity model) errors are not accounted for in these errors.

In 2014, with the goal of identifying earthquakes smaller than M_L 2.1 in the BCNC, NRCan installed five temporary seismometers within the BCNC (Figure 4). It is expected that these new stations will aid in locating small earthquakes in

the BCNC that were not previously detected on the CNSN network. It is anticipated that these stations will also decrease the errors associated with event locations in region.

Currently there are two velocity models that are used in earthquake location solutions in the BCNC. West of -130° , velocity model cn06 is used, while east of -130° velocity model cn01 is used. CN06 is a multi-layered model that allows for depth calculations, while cn01 is a two-layer (35-km-thick layer over a half space), one-dimensional model that does not allow for depth calculations (Mulder, 2005). The majority of solutions in the BCNC have depths fixed at 1, 5, 10, or 18 km; however, there are some depths that were not set by an analyst.

Due to the low quantity of moderate-to-large earthquakes in the BCNC there are no focal mechanisms available to describe the local stress regime in this area. Southeast of the BCNC there is one focal mechanism, derived from a M_L 4.3 event on June 10, 2004 that occurred within the Anahim Volcanic Belt (Figure 1&4). This event has a strike-slip mechanism, while a M_L 3.4 event south-east of the target area shows a dipping strike-slip mechanism. To the west, events in Hecate Strait show a combination of thrust and strike slip mechanisms. These mechanisms agree with the overall NE-SW orientated compressional regime in western Canada (Ristau et al., 2007).

GPS Monitoring and Data

Prior to 2014 there were two permanent, provincial (BCPR-Prince Rupert, and BCTE-Terrace) GPS stations and no GSC-operated GPS (global positioning system) sites in the BCNC (Figure 1,3&4). BCPR has frequent data gaps and the installation of the BCTE pier is unstable, both resulting in low data quality at the respective sites (M. Schmidt, pers. com., 2013). The Canadian Base Net (CBN) has GPS piers in place in Smithers (SMIT) and Bella Coola (BLBC); however, instrumentation upgrades and equipment were needed to bring these stations on-line. West of the BCNC there is a permanent GPS site located in Sandspit (BCSS), which has been recording data since 2005 in addition to temporary GPS sites on Haida Gwaii (deployed following the October 28, 2012 M_w 7.8 Haida Gwaii earthquake). To the north and south of the target area the closest continuous GPS stations are located at Dease Lake, approximately 550 km north of Terrace, and at Port Hardy on northern Vancouver Island, respectively. Supplementing the continuous GPS sites, there are many campaign sites in BC that have been occupied for short periods at various times since 1993 (Hippchen, 2011). The closest campaign sites to the BCNC are KING (~40 km south of Bella Bella), and a number of sites on Haida Gwaii.

The combination of continuous and campaign GPS data have resulted in knowledge of the general crustal deformation rates with respect to stable North America in the ITRF2000 (Altamimi et al., 2002) reference frame in the BCNC; however due to the gap of GPS studies in the BCNC, local deformation rates and vectors within the BCNC cannot be accurately resolved. Studies adjacent to the target area have shown that to the west, on Haida Gwaii, deformation rates range from 9.2-18.8 mm/a NOW-N25W (Hippchen, 2011; Figure 5). GPS measurements to the south of the target area, within northern Cascadia, show rates of 1-10 mm/a (increasing in a westerly direction towards the coast) orthogonal to the JdF/NA plate margin, with an uplift of ~2 mm/a (Mazzotti, et al. 2003a; Figure 5). Between these two regions (northern Vancouver Island and the adjacent mainland) has been defined as a transition zone, where deformation rates are much lower (1.8-5.2 mm/a) and the vectors rotate from N at the northern stations to NW at the southern stations (Hippchen, 2011; Figure 5). GPS measurements across northern BC, southern Alaska and the Yukon Territories reveal crustal velocities on the BC/Alaska coast of 10.8 mm/a NW (dominated by motion on the Fairweather Fault) and additional inland deformation rates up to 3 mm/a NE due to the Yukutat collision (Leonard et al., 2007). From these regional studies GPS velocities at Prince Rupert, Terrace and Smithers were calculated to be 4.93, 2.61 and 1.60 mm/a N-NW, respectively (Hippchen, 2011). These results suggest that there may be some strain being transferred to the BCNC from tectonic processes to the west and southwest.

Recent aspirations to improve the GPS network in BC include the installation of a permanent GPS pier on Bonilla Island in March 2014, and upgrading instrumentation at the Bella Coola and Bella Bella GPS stations in March 2015 (Figure 4).

Seismic Hazard

Although there are no identified active faults in the BCNC, seismic-related hazards are still a concern. Aside from tsunamis, damage related to earthquakes is primarily an effect of the shaking induced by earthquakes. For this reason, defining hazard as the likelihood of exceeding a given ground shaking level, as opposed to relating it to the magnitude of an earthquake, is more applicable when assessing hazard. Ground shaking Intensity Measures (IMs) can be reported as PGA (peak ground acceleration), PGV (peak ground velocity), S_a (spectral acceleration), as well as Macroseismic Intensity (based on modified Mercalli intensity, MMI). PGA and PGV refer to the peak level of ground motion, S_a refers to the maximum response of a harmonic oscillator at a specific period (T) to ground motion, and MMI is an assigned value based on physical impacts to the built environment and the perceived shaking felt by humans (Wood and Neuman, 1931). PGA and S_a are reported in units of cm/s^2 , or in terms of g or $\%g$, where g is acceleration due to gravity (981 cm/s^2). PGV is often reported in units of cm/s . MMI is reported by a qualitatively assigned number between I-XII, which corresponds to different levels of felt shaking and observed damage. Many relationships between MMI and PGA have been published (e.g. Cua et al., 2010). A recent relationship, derived from joint probabilities of California Did You Feel It? and strong-motion data was published by Worden et al. (2012). An older relationship that has been frequently used and is seen in publications is from Wald et al. (1999). Slight differences between the two are seen at $\text{MMI} \leq V$ (Worden et al., 2012).

There are two approaches that are commonly used to assess seismic hazard; probabilistic and deterministic. Probabilistic seismic hazard analysis (PSHA) quantifies the uncertainties of location, size and resulting shaking due to all possible earthquakes at a specific location. Deterministic seismic hazard analysis models a specific earthquake scenario to estimate ground motion levels due to a specified earthquake rupture. Both methods involve assumptions, therefore neither approach will predict the exact ground motions that will occur at a site, nor will they guarantee that a more complex earthquake scenario not included in the hazard assessment will occur.

Probabilistic Seismic Hazard Assessment

Probabilistic seismic hazard assessment sums the total seismic hazard in an area and is crucial input to building codes, community planning and emergency preparedness. NRCAN publishes its Seismic Hazard Maps of Canada approximately every five years. Using the hazard calculator provided by Earthquakes Canada (http://www.earthquakescanada.nrcan.gc.ca/hazard-alea/interpolat/index_2010-eng.php), probabilistic hazard values used in the 2010 National Building Code of Canada (NBCC, 2010) can be determined at specific locations (note that at the time of this study 2015 seismic hazard values were not published. All PSHA values in this report are from the 2010 Canadian Seismic Hazard Map). Using this tool the ground shaking levels that have a 2% probability in a 50-year period of being exceeded (e.g. a one in 2,475-year shaking event) were determined for a range of locations throughout the BCNC. The highest shaking levels are expected along the West Coast of the BCNC (PGA 0.184 g), decreasing to the very eastern extent of the Coast Mountains (PGA 0.172 g). In terms of S_a for the same probability level, expected shaking at shorter periods [$S_a(0.2)=0.364-0.388 \text{ g}$] are generated from local earthquakes, while longer-period motions [$S_a(2.0)=0.072-0.093 \text{ g}$] are generally generated from distant earthquakes (see table 2).

The NBCC, 2010 seismic hazard values are based on NEHRP 'site class C' foundations (Finn and Wightman, 2003). This assumes the time-averaged shear wave velocity in the upper 30 m is 360-750 m/s. Softer soils (class D-E) are known to experience higher levels of ground motion for a longer duration than hard rock (class A-B). If the site conditions differ

from 'site class C', the amount of shaking expected at that site (according to 2010 NBCC) will change by the corresponding foundation factor (F_a) in Finn and Wightman, 2003 (Table 3).

While the PSHA provides a probabilistic sum of hazard from the combination of all plausible earthquake scenarios that are likely to occur, sometimes an assessment of the individually contributing seismic hazards is desired. GSCFRISK (a tool modified from FRISK88, proprietary software from Risk Engineering Inc.) was used to deaggregate the PSHA to obtain the predominant sources of seismic hazard at a central location (53.5N, 129.0W) in the BCNC (S. Halchuk and A. Bent, pers. comm., 2013). The results of the deaggregation are presented graphically as 3D bars that proportionally represent the magnitude and corresponding distances from the specified location of earthquakes that contribute to exceeding the ground-motion hazard at that location. The mean and modal magnitude and distance of the contributing earthquakes is also output. Deaggregations were calculated for a 2%/50 PE for the mean, median and 84th percentile of the seismic hazard for different spectral periods ($T = 0.2, 0.5, 1.0, 2.0$ s), as well as PGA. The results of the deaggregation of the 84th percentile of the hazard are shown in Figure 6.

For shaking with periods ≥ 1 s the predominant hazard is from earthquakes of $M_L > 6.75$, 300-350 km away (Figure 6). Approximately 300 km west of the BCNC lies Haida Gwaii (Figure 1) which has experienced four nearby earthquakes greater than $M_L 7$, and 14 events between $M_L 6-7$ (from CNSN archives). To the southwest of the BCNC, within the 300-350 km range is the northern portion of the CSZ (Figure 1), which has the potential to experience an earthquake with ground motions similar to the March 11, 2011 $M_w 9.0$ Tohoku-Oki, Japan or the March 27, 1964 $M_w 9.2$ Alaska earthquakes. Similarly, south-eastern Alaska (Figure 1) has also experienced earthquakes greater than $M_L 6.75$ (Page et al., 1991), which may contribute to the long period seismic hazard in the BCNC.

The seismic hazard for shorter periods (< 1 s) is highest at distances < 300 km and is dominated by smaller local sources (Figure 6). These results confirm that local sources contribute towards the short-period hazard, while large, distant earthquakes dominate the long-period hazard.

Deterministic Hazard Assessment

While PSHA can determine the mean or some fractile (i.e. 50th, 84th, etc) of possible shaking in an area considering all possible sources, a deterministic approach calculates IMs using attenuation relationships based on a specific earthquake scenario. The USGS software ShakeMap (Wald et al., 1999a&b) calculates PGA, PGV, $S_a(0.3)$, $S_a(1.0)$, $S_a(3.0)$ using site conditions derived from the topographic gradient (Wald and Allen, 2007; Allen and Wald, 2009). The calculated ground motion is then converted to MMI based on relationships determined by Worden et al. (2012). From the calculated shaking IMs areas susceptible to high levels of shaking due to specific, theoretical earthquakes can be highlighted.

ShakeMap was used to calculate shaking IMs for three known potential scenarios near the BCNC as determined by deaggregation results and past seismicity; 1) a $M_w 8.0$ shallowly-dipping subduction event on the Haida Gwaii thrust; 2) a $M_w 7.2$ strike-slip event on the newly mapped feature in the Douglas Channel (Figure 1), and; 3) a $M_w 6.3$ event near the epicentre of the 1973 Terrace earthquake. The magnitudes of the scenario earthquakes were determined from rupture area-to-magnitude scaling relations. For shallow crustal earthquakes, the average magnitude of five scaling relationships was used (Wells and Coppersmith, 1994; Hanks and Bakun; 2002; Reasenberget al., 2003; Shaw 2009; Leonard, 2010), while Strasser *et al.* (2010) was used for subduction earthquakes.

Haida Gwaii Thrust Earthquake $M_w 8.0$

A plausible maximum magnitude predicted on the Haida Gwaii thrust fault (by the method mentioned above) is $M_w 8.0$, based on the estimated fault area (Strasser *et al.*, 2010). This scenario is three-tenths of a magnitude unit larger (approximately a factor of two in fault area) than the October 28, 2012 (UTC) $M_w 7.8$ Haida Gwaii earthquake, which the

average of the reported community decimal intensities (CDI, Dengler and Dewy, 1988) was 6.0 (Bird and Lamontagne, 2015). The maximum estimated shaking intensity for this scenario is 0.91 g, which occurs offshore, 60 km west of Haida Gwaii. Shaking intensities upwards of MMI VIII, or PGA=0.6 g would be expected on the west coast of Haida Gwaii, diminishing to MMI III or PGA=0.005 g along the eastern extent of the BCNC (Figure 7a). Based on the assumed ground-motion attenuation model (Zhao et al., 2006), little-to-no damage to low-rise (short-period) structures would be expected in the BCNC. Damages on Haida Gwaii would be at minimum, similar to what was observed in 2012 (for details of damage see Bird and Lamontagne, 2015).

As deaggregation results suggests, a portion of the modelled seismic hazard in the BCNC is due to long duration, long period waves from earthquakes more than 300 km away (Figure 6), such as a large earthquakes offshore Haida Gwaii. Significant long-period, long duration shaking from such an event may affect taller structures and trigger ground failure (i.e. liquefaction or lateral spreading) in areas with sensitive soils. Inspecting the Sa(1.0) and Sa(3.0) results of the Haida Gwaii thrust scenario (Figure 7b) indicates that shaking in Kitimat resulting from periods of 1.0 s and 3.0 s is estimated to be 0.037 g and 0.013 g for a median event, respectively. Along the coastal islands, estimated shaking more than doubles to approximately 0.10 g and 0.03 g, (at $T=1.0$ s and 3.0 s respectively).

Douglas Channel M_w 7.2

This scenario (Figure 7c) is based on the rupture of a recently mapped fault-like structure in the Douglas Channel (Figure 1; Conway et al., 2012). Based on published fault-scaling relations (e.g. Wells and Coppersmith, 1994; Hanks and Bakun, 2002) if the entire fault (~60 km) ruptured in a strike-slip event an earthquake of approximately M_w 7.2 could be expected. Estimated MMI from such an event would be very strong (VII-IX) within 20 km of the fault, decreasing to MMI III at distances at the outer boundaries of the BCNC (Figure 7c). Very little damage would be expected for most of the BCNC; however, moderate to heavy damage would be expected within 20 km of the rupture. The expected effects and impacts of such an earthquake would mimic those of the 1946 M_w 7.3 Vancouver Island earthquake, which occurred slightly west of Courtney and Campbell River. Shaking due to the 1946 earthquake was felt as far as Prince Rupert, BC to the north and Portland, Oregon to the south. In addition to knocking down 75% of the chimneys in the local area, much of the earthquake-related damage was due to landslides, slumping and liquefaction (Mathews, 1979; Rogers, 1980; Slawson and Savage, 1979). Potential impacts of earthquake-triggered ground failure for this scenario will be addressed in the next section.

Terrace M_w 6.3

On May 11, 1973 a M_w 4.7 shallow crustal earthquake approximately 20 km south of Terrace shook nearby communities and was felt as far as 120 km away. In Terrace the maximum reported shaking intensity was MMI V. Damage included a few broken windows and some cracked plaster (Rogers, 1976). The event has not been associated with any geologic features in the area and little is known about its rupture process. The Terrace ShakeMap scenario (Figure 7d) estimated shaking IMs for a slightly larger earthquake (M_w 6.3) in the same estimated location as the 1973 event. This scenario estimates strong to very strong shaking in Terrace (MMI VI; PGA=0.26 g), light-to-moderate shaking (MMI IV; PGA=0.05 g) near Kitimat, and shaking IM's as low as MMI III and PGA=0.009 g in other areas of the BCNC (Figure 6b). Based on the predicted MMI for this scenario damages would likely be constrained to a ~20 km radius around the epicenter.

Seismically-Induced Ground Failures

Although the actual shaking caused by an earthquake can be detrimental to buildings and terrifying to humans, there are secondary consequences of earthquake shaking that can be equally or more devastating. Ground failures, a common result of earthquake shaking, can have widespread negative effects on lives, vegetation, wildlife habitats, and

infrastructure. Ground failures triggered from earthquake shaking fall into three categories: 1) disrupted slides and falls, 2) coherent slides, and 3) lateral spreads and flows (Keefer, 2002). Disrupted falls include landslides consisting of boulders, rock fragments, blocks of soil, and falling, rolling or bouncing rocks and soil grains. Disrupted falls originate on steep slopes and travel fast and far beyond the base of the slope. Coherent slides describe translational or rotational slides and slumps and slow earth flows. Coherent slides usually occur on moderately steep slopes and move slowly. Both coherent and disrupted slides introduce an additional level of hazard because they are capable of generating damaging tsunamis if they run out into a body of water. Lateral spreads and flows include any ground failure (although little slope is required) that has fluid-like movement due to high levels of water in the sediments involved. Included in the lateral flows and slides category are liquefaction and submarine landslides (Keefer, 2002).

Reviews of historical seismically induced ground failures (Keefer, 1984; Rodriguez, 1999; Keefer, 2002) reveal characteristics and relationships of ground failures and a number of seismic, geologic and environmental parameters. General conclusions of these reviews include: 1) The most common areas to be impacted by ground failure have surface lithology composed of any material that is naturally weak (sands, tills, clays), or has been weakened by natural or unnatural processes, 2) Earthquake induced ground failures in the form of lateral spreads and flows, soil avalanches, and disrupted slides can occur in areas with slopes as small as 0.3°, 5°, and 15°, respectively, 3) Different types of ground failures have different threshold magnitudes and shaking intensity. While the threshold for a disrupted fall is $M 4.0/$ MMI IV, the threshold for coherent slides is $M 4.5/$ MMI V and for lateral spreads and flows is $M 5.0/$ MMI V. Based on MMI/PGA relationships (Worden et al., 2012) these shaking intensities are equivalent to PGA of approximately 0.028 g (disrupted slides) and 0.062 g (coherent slides and lateral spreads and flows), 4) The distance away from the rupture and area affected by earthquake triggered landslides increases with magnitude. Based on observed earthquake-triggered ground failures, for a $M9+$ earthquake the greatest distance from a fault rupture that a landslide is expected is 250 km (Keefer, 2002).

The level of hazard that earthquake-triggered ground failures impose on an area depends on a number of physical factors, as well as the ground shaking level and duration, which are a function of the earthquake rupture process, and the path the waves take from the source to the surface (Fry et al., 2011). Prominent physical factors include: slope angle, aspect, curvature and height, precipitation, permafrost, surface and bedrock geology, vegetation and distance to water bodies (Miles and Keefer, 2009; Dominguez and Bobrowsky, 2011). In general, the greater the slope, curvature, precipitation and permafrost, and the closer to water bodies, the higher the landslide susceptibility (Dominguez and Bobrowsky, 2011). As previously mentioned, in most cases, the larger the magnitude of an earthquake, the larger the possible landslide area and the more landslides it will trigger. However, due to varying geologic and seismic conditions as well as incomplete databases, the number of recorded landslides can vary greatly between events of the same magnitude.

Included in the third type of ground failure, as defined in Keefer (2002) is liquefaction. Liquefaction occurs when shaking re-orientates sediments so that they take up less space and water is forced out of the pore space. This results in a loss of sediment strength such that sediments act fluid-like. Any overlying layers or infrastructure will float on this now liquefied sediment, resulting in lateral spreading and fracturing in the form of sand boils and fissures (Kayen et al., 2004). Although long period seismic waves contribute most to liquefaction hazards, correlations between S_a or PGV and liquefaction are not frequently reported. The period of seismic waves recorded near liquefaction sites range from less than 1 s to 10's of seconds (Wang and Manga, 2010), however; studies show that liquefaction is most responsive to lower frequency (0.2-2.3 Hz) ground shaking and depends more on the shaking duration than on short pulses of high acceleration (Seed and Lee, 1966; Wong and Wang, 2007; Wang and Manga, 2010). In the case of the 1999 $M_w 7.5$ Chi Chi earthquake, liquefaction was documented at sites that measured $S_a(1.0) > 16 \text{ m/s}^2$ and $S_v(1.0) > 2.4 \text{ m/s}$ (Wang et al,

2003). A more common correlation is made between liquefaction and PGA. PGA data gathered from recent large earthquakes that have resulted in liquefaction [e.g. 2010 M_w 7.0 Haiti (Olsen et al., 2011); 2010 M_w 7.1 and 2011 M_w 6.3 and M_w 6.0 Christchurch (Cubrinovski et al., 2011); 1999 M_w 7.5 Chi Chi (Wang et al., 2003; Wong and Wang, 2007)] reveal that without taking into account site conditions, if $PGA > 0.1$ g liquefaction may occur.

In addition to information about the frequency and duration of shaking, local soil characteristics need to be considered when determining areas prone to liquefaction. Areas with younger, more fine-grained soil with a high water table will be more prone to earthquake-triggered liquefaction (Saunders and Berryman, 2012). Empirical relations between the level of ground shaking and liquefaction (such as Arias intensity (Arias 1970) and Cumulative Absolute Velocity-CAV (Benjamin, 1988; O'Hara & Jacobson, 2006) may be combined with numerical simulations of ground shaking during an earthquake to evaluate the liquefaction susceptibility of large areas. These simulations require extensive information about sediment properties and subsurface structures which are often unavailable. A simpler approach based on empirical data that may be applied to set limits on the expected extent of liquefaction during earthquake is: $\log R_{\max} = 2.05 (\pm 0.10) + 0.45M$, where R_{\max} is the distance from the hypocenter and M is the Magnitude (Wang et al., 2006).

Although less frequently reported due to their remote, underwater locations, submarine landslides impose a significant hazard to populations near bodies of water. While most submarine slopes are considered stable, external effects such as shaking due to earthquakes and construction, or increased sedimentation which have the ability to increase pore pressures may trigger slope failure. As pore pressures increases, the frictional resistance to sliding between sediment layers will decrease, weakening the layers and resulting in movement between them. Due to the submarine environment, submarine ground-failures also have potential to generate turbidity currents and tsunamis which can affect lives and infrastructure for hundreds of kilometers (Masson et al., 2009, Locat and Lee, 2002).

BCNC Ground Failures

A preliminary 1:6 million scale landslide susceptibility map of Canada (Dominguez and Bobrowsky, 2011; Figure 7) based on digital databases describing precipitation, permafrost distribution, bedrock lithology, elevations and distance from rivers and coasts has been produced by NRCan. To establish the relevance the mentioned variables have to landslide hazard each parameter was divided into a number of classes (by GSC landslide experts) based on their tendency to increase ground failures. Overall landslide susceptibility for an area was determined by the combination of classes (which reflect the susceptibility of that parameter) the area fell into. On a scale of 1 to 6 (6 representing the highest susceptibility), the majority of the west coast of BC exhibits landslide susceptibility values of 5-6, which is significantly higher than the rest of Canada (Bobrowsky and Dominguez, 2012).

Jakob et al. (2006) and Geertsema et al. (2005) describe a number of non-earthquake-triggered ground failures in northern BC over the past three decades. Impacts of these landslides include damage to pipelines, rail, and forestry, as well as fish habitats. Most of the events were triggered by delayed melting of the annual snow pack, heavy rains, bank erosion and site loading and caused long-lasting damming of the rivers they flowed into (Geertsema et al., 2005). Although no events in the BCNC are known to be seismically induced, the existence of numerous landslides strengthens the likelihood of seismically induced ground failures occurring in the BCNC. Due to the high levels of seismicity surrounding the BCNC (Figure 1), it is expected that the increased likelihood of strong ground shaking (with long durations) will increase the landslide susceptibility. Software that calculates the hazard of seismically induced landslides (Lee et al., 2008, Miles and Keefer, 2009; Godt et al., 2008) is starting to become popular, but has not yet been implemented in Canada.

Within the BCNC there has been one documented tsunamigenic, non-earthquake triggered submarine slope failure near Kitimat (Figure 1; discussed earlier). More recently, Conway et al. (2012) documented an additional two significant submarine slope failures in the Douglas Channel that were possibly triggered by movement on a suspected nearby fault. The absence of earthquake records makes it difficult to determine exactly how these slope failures were triggered. These submarine slides are approximately 15 km from the recently mapped fault-like feature in the Douglas Channel fault (Figure 1). According to simple distance/magnitude relationships from Keefer (2002), the smallest earthquake that could have triggered these landslides at a distance of 15 km is M 5.8. Detailed land and marine-based studies are required to determine if this feature and the submarine slides are related.

The 2%/50-year probabilistic PGA (based on NBCC, 2010) in the BCNC is between 0.17-0.18 g (table 2). Shaking of this level is equivalent to MMI VI-VII and would cause light to moderate damage and has the capacity to trigger all types of ground failure. This estimate is not based on a specific earthquake, and does not take into consideration site conditions, which would alter the shaking response. Earthquake-induced ground shaking is often amplified in areas with significant impedance contrasts, such as soft, low-velocity sediments overlying stiff bedrock. In this setting, the impedance contrast causes a shortening of shear-wave wavelengths and an increase in shear-wave amplitudes (Shearer and Orcutt, 1987; Hunter and Crow, 2012). This amplification can be escalated when shear waves become trapped in the low-velocity soil zone and 'ring' at the fundamental frequency (f_0) and subsequent harmonics until the energy eventually dissipates. Maximum shaking IMs (PGA/MMI) obtained from ShakeMaps for a M_w 8.0 Haida Gwaii thrust event, a M_L 6.3 event near Terrace, and a M_w 7.2 strike-slip event along the suspected fault in the Douglas Channel are 0.91 g/8.75, 0.26 g/6.93, and 0.95 g/8.53 (respectively). Shaking IMs of these levels have the ability to cause light to very heavy damages and have the potential to trigger all types of ground failure. For both the probabilistic and deterministic hazard assessments, ground failures would most likely be concentrated in susceptible areas with either high slopes or weak sediments. These conditions are commonly found along valleys and channels in the BCNC.

The largest contribution to the hazard that a large Haida Gwaii earthquake imposes to the BCNC is long duration, long period ground shaking. Within the study area the maximum 2%/50-year probabilistic seismic hazard for $S_a(1.0)$ and $S_a(2.0)$ is 0.163 g and 0.093 g, respectively. ShakeMap predicts shaking IMs for the M_w 8.0 Haida Gwaii scenario of approximately $S_a(1.0)=0.09$ g and $S_a(3.0)=0.03$ g (Figure 7a,b) along the west coast of the BCNC, which are both lower than the threshold S_a found by Wang et al. (2003). This suggests that a large, distant earthquake, such as a M_w 8.0 Haida Gwaii thrust event would likely not cause any type of ground failure in the BCNC. However, such an earthquake has estimated shaking IMs on Haida Gwaii of MMI VIII, decreasing to MMI III in the eastern Coast Mountains and $PGA \sim 0.6$ g along the west coast of Haida Gwaii decreasing to 0.005 g in the Coast Mountains. Although the Haida Gwaii scenario spectral accelerations in the BCNC are less than any estimated threshold level for ground failure, the scenario PGA and MMI, are both greater than estimated PGA and MMI ground failure threshold levels given by Keefer (2002).

Although the estimated S_a and PGA do not exceed threshold ground failure levels, for the M_L 6.3 Terrace earthquake scenario, the predicted MMI ranges from III in the majority of the study area to VI near Terrace and MMI V-VI near Kitimat. Shaking IMs of MMI V have been known to trigger ground failures (Keefer, 2002). Given this, it is plausible that an earthquake similar to the 1973 M_L 6.3 Terrace earthquake could trigger ground failures in the Kitimat region.

Of all the deterministic scenarios, the Douglas Channel scenario predicted the highest shaking IMs in the BCNC. The fault used in this scenario is based on the topographic and bathymetric relief of the proposed Douglas Channel fault documented by Conway et al., 2012. An earthquake resulting from a rupture along the full length (60 km) of this fault could be as large as M_w 7.2. The maximum PGA and MMI are 0.95 g and 8.53, respectively. As expected, the shaking IMs for this event are highest near the hypothetically ruptured fault trace and diminish to MMI III at the edges of the study

area. The shaking IMs predicted for this event could cause ground failures as far as 150 km away, possibly affecting an area upwards of 5000 km² (Keefer, 2002). The submarine slope failures observed by Conway et al. (2012) are approximately 15 km away from the northern end of the fault. Observations of previous earthquake-triggered submarine slides reveal that these slides could have been triggered by earthquakes as small as M 5.8 on the recently mapped structure in the Douglas Channel.

Although it has been determined that shaking levels are more highly correlated with earthquake-triggered landslides than the earthquake magnitude, empirical relationships between shaking and landslides have not been published. $PGA > 0.1$ g is a general threshold for landslides (Olsen et al., 2011; Fry et al., 2011; Saunders and Berryman, 2012), while $S_a(1.0) > 1.6$ g (Wang et al., 2003) has been correlated with seismically-induced liquefaction. Since local geology and ground conditions are controlling factors in determining areas susceptible to liquefaction, ground-motion threshold relationships for the local area would be more meaningful. Due to the many factors that determine the locality of earthquake-triggered landslides, without more detailed studies of the local geology and soil conditions, the determination of local landslide susceptibility in the study area is presently difficult. As observed in the 1988 M_w 5.9 Saguenay earthquake, the presence of clays (like those in the Kitimat Valley) can amplify ground shaking and secondary effects of it (Rodriguez, 1999; Brooks, 2013).

Conclusions

The Coast Mountains form the west coast of North America from Alaska to southern BC. The section of this mountain range from Prince Rupert south to Bella Bella is an area of potential future growth, which will have significant societal and economic impacts to the region. The random nature of natural hazards poses a risk to coastal communities and developments, and therefore the economy in this growing region. As part of the Public Safety Geoscience Program, a mandate of the Geological Survey of Canada is to monitor, investigate and report on natural geological hazards (such as earthquakes and landslides) occurring in, or having the potential to negatively impact Canada. The objective of this study was to collect existing data regarding natural geohazards in the BCNC and identify knowledge gaps therein.

As the PA plate continues to converge with the NA plate, deformation of both plates endures – with minor observable consequences in the BCNC. Relative to the rest of Canada's West Coast, the BCNC has experienced fewer historical earthquakes which resulted in a scarcity of earthquake monitoring instrumentation and research in the BCNC. Prior to 2014 there were four permanent seismographs bordering the BCNC allowing for a $M_c = 2.1$. Although this is a vast improvement compared to before 2007, this M_c is still 0.5-1.0 units of magnitude higher than the well-instrumented south-west BC. With the addition of five new temporary seismographs installed in 2014, the M_c and accuracy of earthquake locations in the BCNC will improve.

Prior to 2014 there were two provincial GPS sites operating in the BCNC; both of which have low data quality. Since 2014 eight additional GPS stations have been brought on-line. Results from previous regional GPS studies suggest that there may be some strain being transferred to the BCNC from adjacent tectonic processes. The additional GPS stations will improve knowledge of the local strain in the BCNC.

Augmenting the existing seismograph network with additional stations increases the ability to identify patterns of small-magnitude earthquakes in the region. A more complete earthquake database along with improved crustal deformation rates (using additional GPS data) for the BCNC will greatly improve our knowledge of seismic hazard in the region.

Whilst there are likely to be many unidentified earthquake sources in the BCNC with varying levels of activity and recurrence, three possible earthquake scenarios that could have negative impacts in the region have been modelled

deterministically; a M_w 8.0 Haida Gwaii thrust event; a M_w 6.3 earthquake near Terrace; and a rupture of the recently mapped Douglas Channel fault-like structure. According to the Earthquakes Canada hazard calculator, 2010 NBCC values a 2% exceedance probability in a 50-year PGA of 0.18 g is estimated along the West Coast, decreasing slightly to approximately 0.17 g on the eastern extent of the Coast Mountains. Deaggregation of the 2010 NBCC shows the predominant short period seismic hazard is from earthquakes in the BCNC <300 km away. Although earthquakes of $M_L > 6.75$, 300-350 km away, along the PA-NA plate boundary still contribute to the long period seismic hazard of the BCNC.

Using a deterministic approach to calculate shaking IMs within the BCNC due to the above-mentioned possible earthquakes, MMI of III-V (Haida Gwaii thrust); III-VI (Terrace); and III-VIII (Douglas Channel fault) are estimated. Shaking IMs of $\text{MMI} \geq \text{IV}$ (Keefer, 2002) and $\text{PGA} > 0.1 \text{ g}$ (Wang et al., 2003; Wong and Wang, 2007; Cubrinovski et al., 2011) have been known to trigger ground failures. Consequently, earthquake-triggered failures are plausible for all of the scenarios presented in this study. At lower MMI, coherent slides and disrupted slides and falls are most probable. As the MMI increases, so does the risk of lateral flows and spreads (i.e. liquefaction). In addition to any ground failures is a range of possible impacts such as human casualties, damage to infrastructure, and triggering of additional hazards such as floods (from damage to waterways and the infrastructure they support) and tsunamis. Specific locations more susceptible to earthquake-triggered landslides cannot be determined from Canada's existing regional landslide hazard map (Bobrowsky and Dominguez, 2012). More detailed mapping is required to specify local areas more prone to ground failure.

A review of existing research prior to 2014 regarding natural geohazards in the BCNC revealed that although regional studies exist, in order to improve the current seismic assessment for this specific region, more knowledge and detailed local research was required. Improved hazard mapping and assessments in the BCNC region required the augmentation of existing monitoring capabilities to provide fundamental baseline data on the occurrence of earthquakes in the BCNC, which has recently been completed. Furthermore, geological studies to target a recently mapped fault-like structure (Conway *et al.*, 2012) are being prioritised. Should this structure be determined to be an active fault, it would pose significant risk of earthquake-triggered landslides (and subsequent tsunami) from the susceptible Douglas Channel hill slopes.

Figures

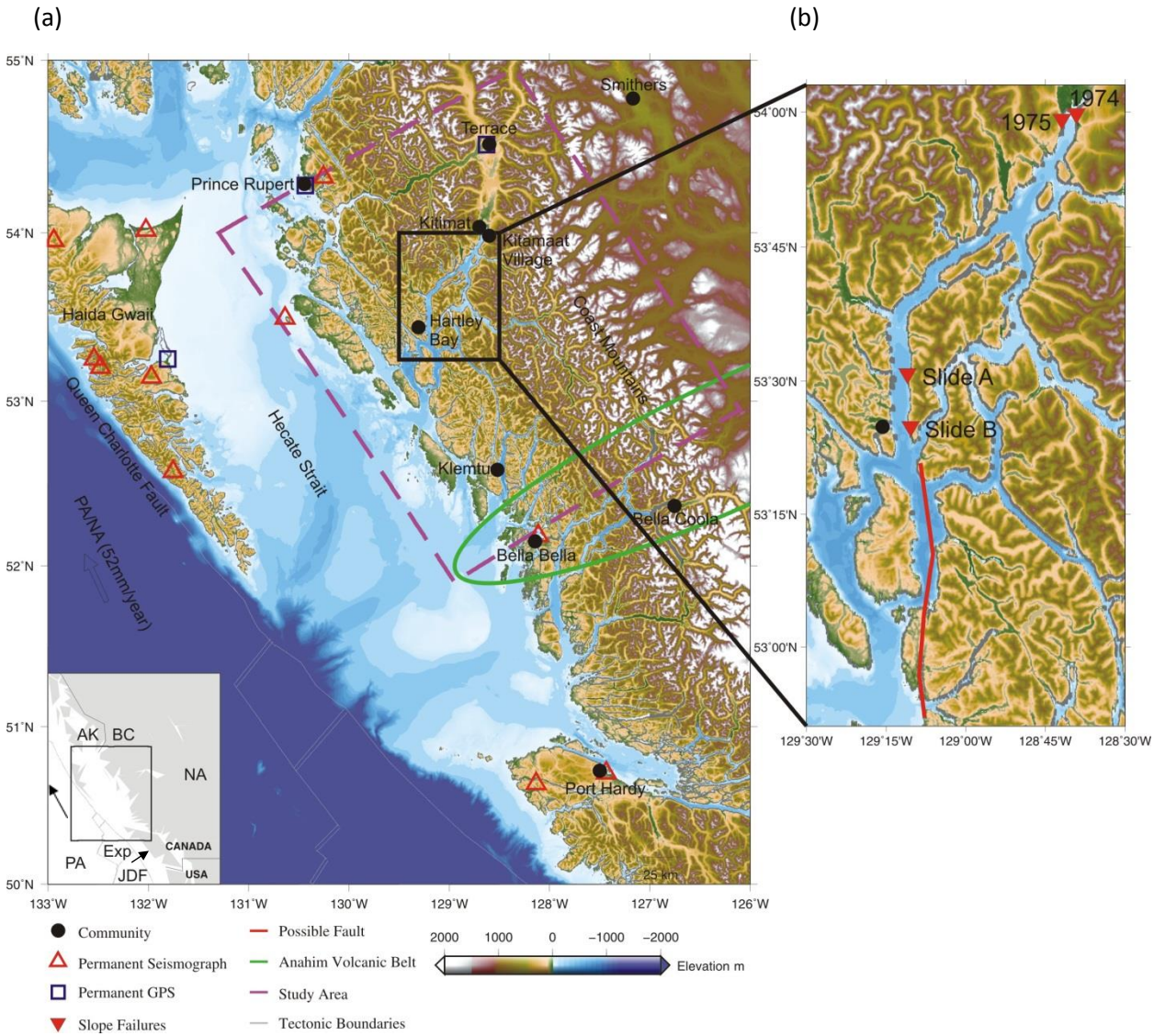


Figure 1 - Location of the BCNC (purple, dashed line). (a) Square within inset shows location of mapped area with respect to tectonic plates and international borders (AK=Alaska, BC=British Columbia, PA=Pacific plate, NA=North American plate, JdF=Juan de Fuca plate, Exp=Explorer plate). Green outline is defines the Anahim Volcanic Belt (b) Known slope failures (inverted triangles) and recently mapped fault (red line) within Douglas Channel as described in (Conway et al., 2012). Slides A and B are submarine slides of unknown dates, 1974 and 1975 mark the subaerial slides that occurred near Kitimat at those respective dates. Colour scheme shows the bathymetry/topography according to the colour scale shown.

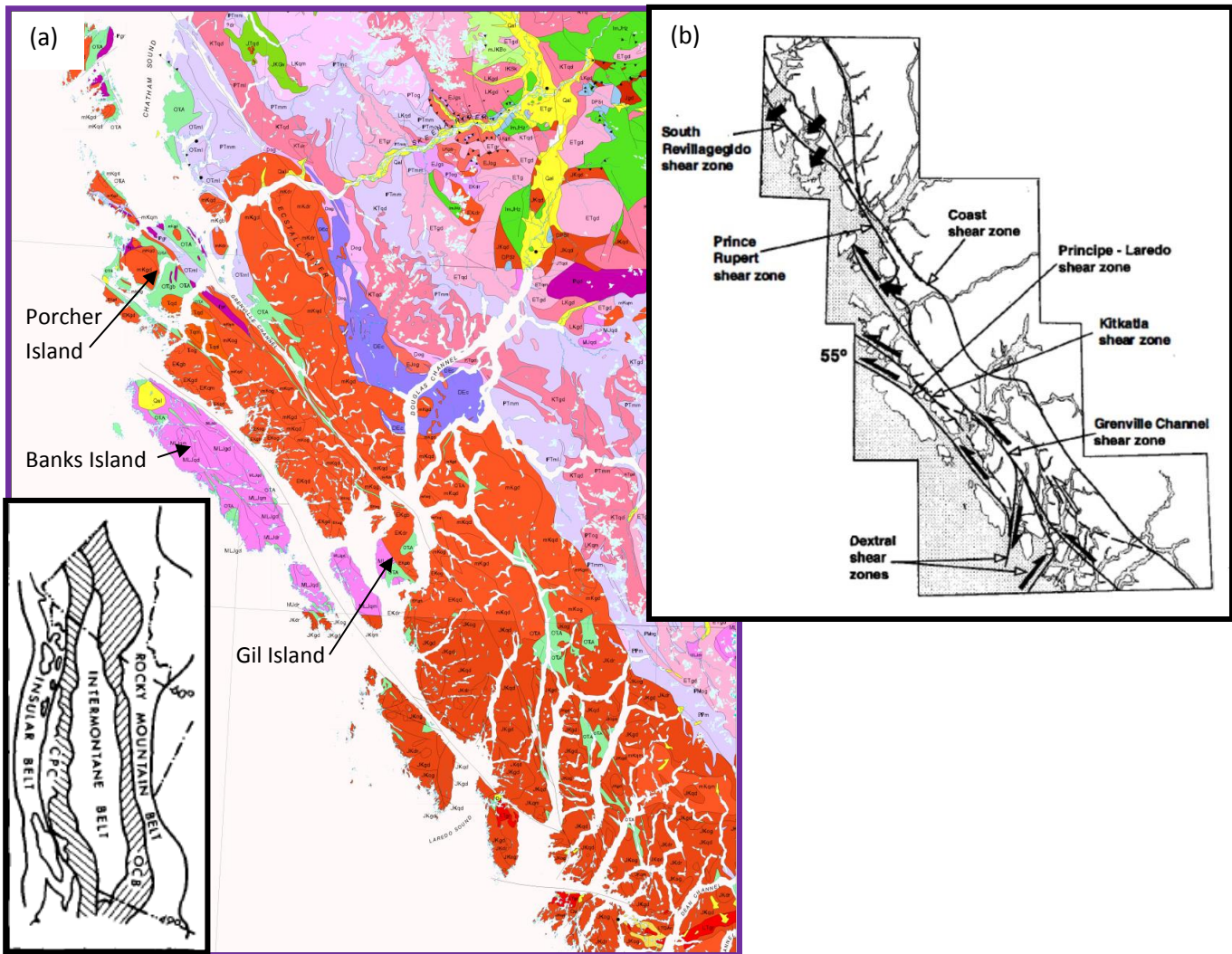


Figure 2 – (a) Orogenic belts of the Canadian Cordillera (inset, from Monger et al., 1982) and local geology near study area. Yellow – Quaternary cover, Dark orange and pink = Mesozoic intrusives, light purples and pinks = Paleozoic intrusives, dark purple = Devonian sediments and volcanics, green = Jurassic sediments and volcanics. A more detailed legend is available in Appendix A. (BC Geological Survey, Geoscience Map 2005-3). (b) Shear zones in BCNC. Arrows show sense of motion (from Chardon et al., 1999).

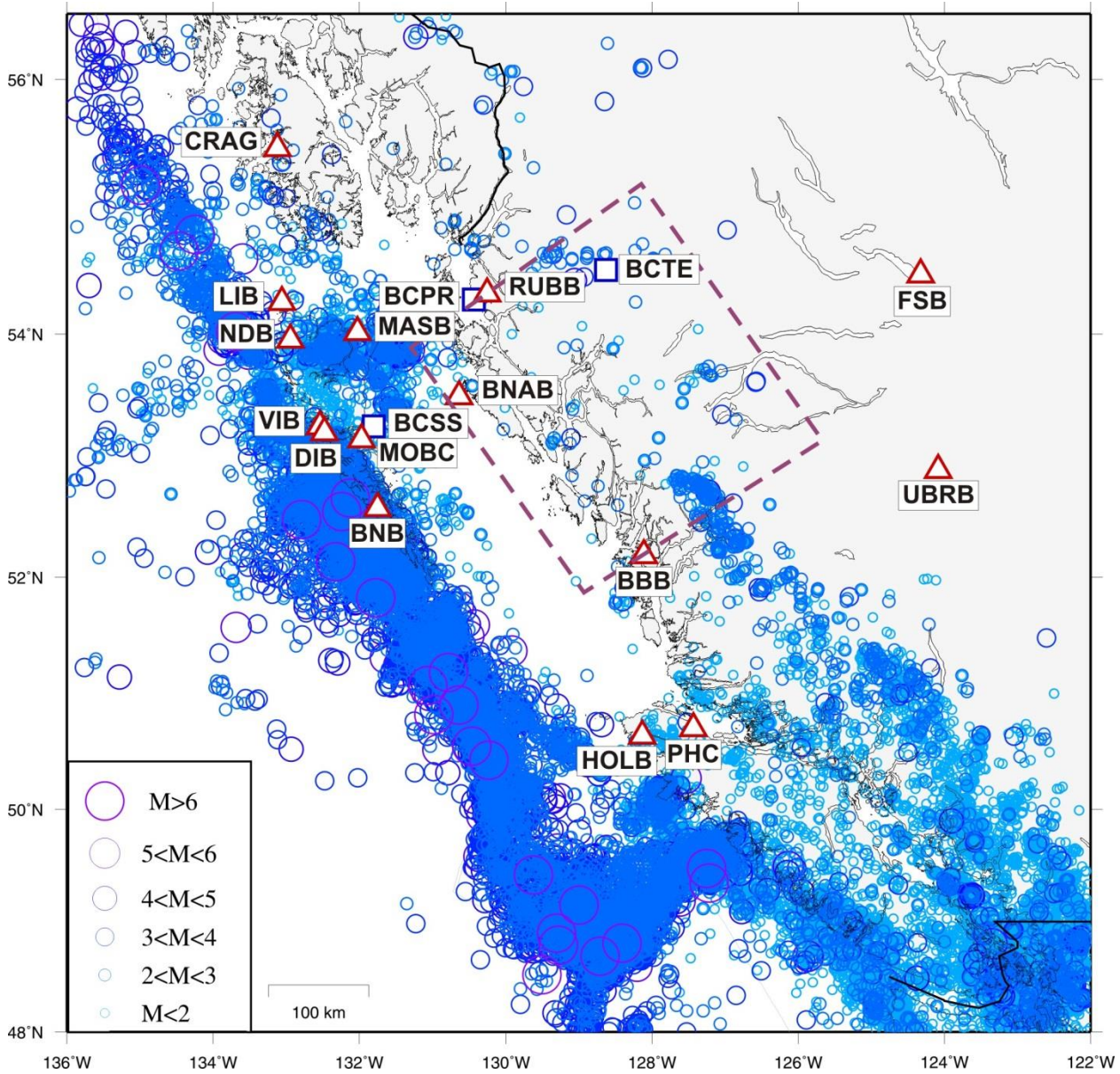


Figure 3 - West Coast seismicity (1971-2013) coloured and scaled by magnitude. Triangles and squares represent seismometers and GPS as in figure 1. Note: Only GPS and seismograph stations used in BCNC earthquake locations are shown.



Figure 4 - BCNC seismicity (1971-2013) coloured and scaled by magnitude (see figure 3a). Shaded areas represent previously identified areas of seismicity (Hecate Strait/Haida Gwaii (blue), Anahim Volcanic Belt (green), possible blasting (orange). Symbols are the same as for figure 1. New or updated stations are labelled (see table 1 for exact locations and start dates).

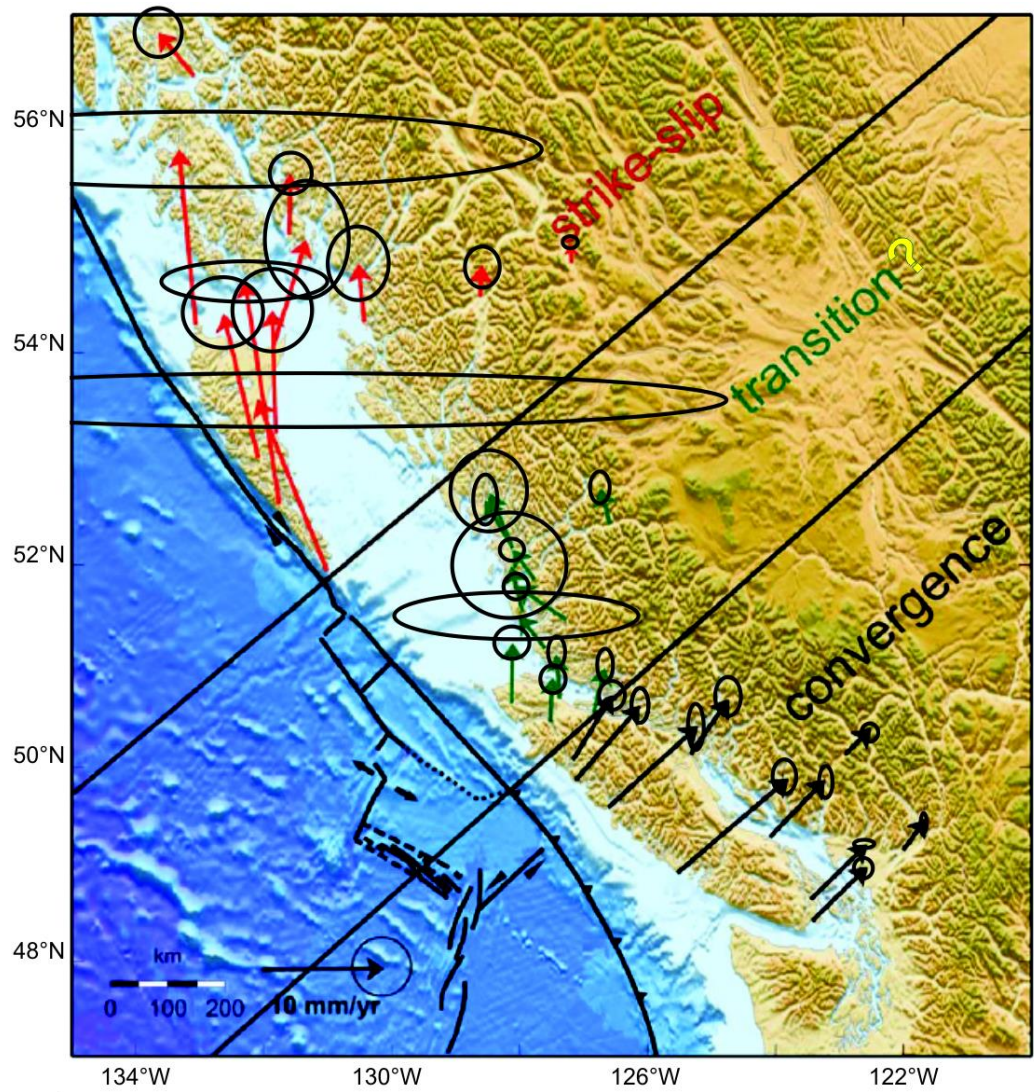


Figure 5 - Horizontal velocity vectors (and approximate error ellipses) from GPS for Haida Gwaii and Vancouver Island areas (after Hippchen, 2011).

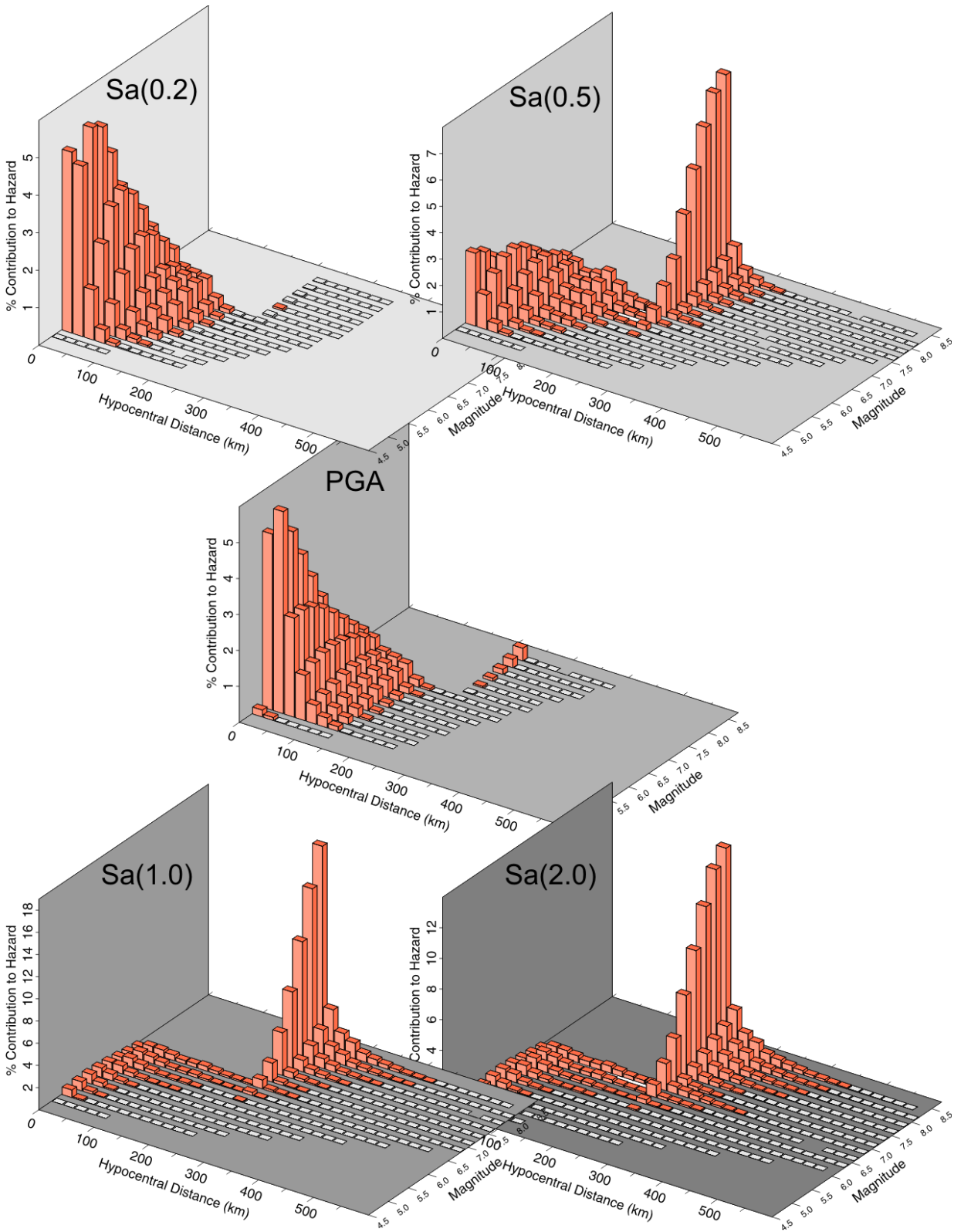
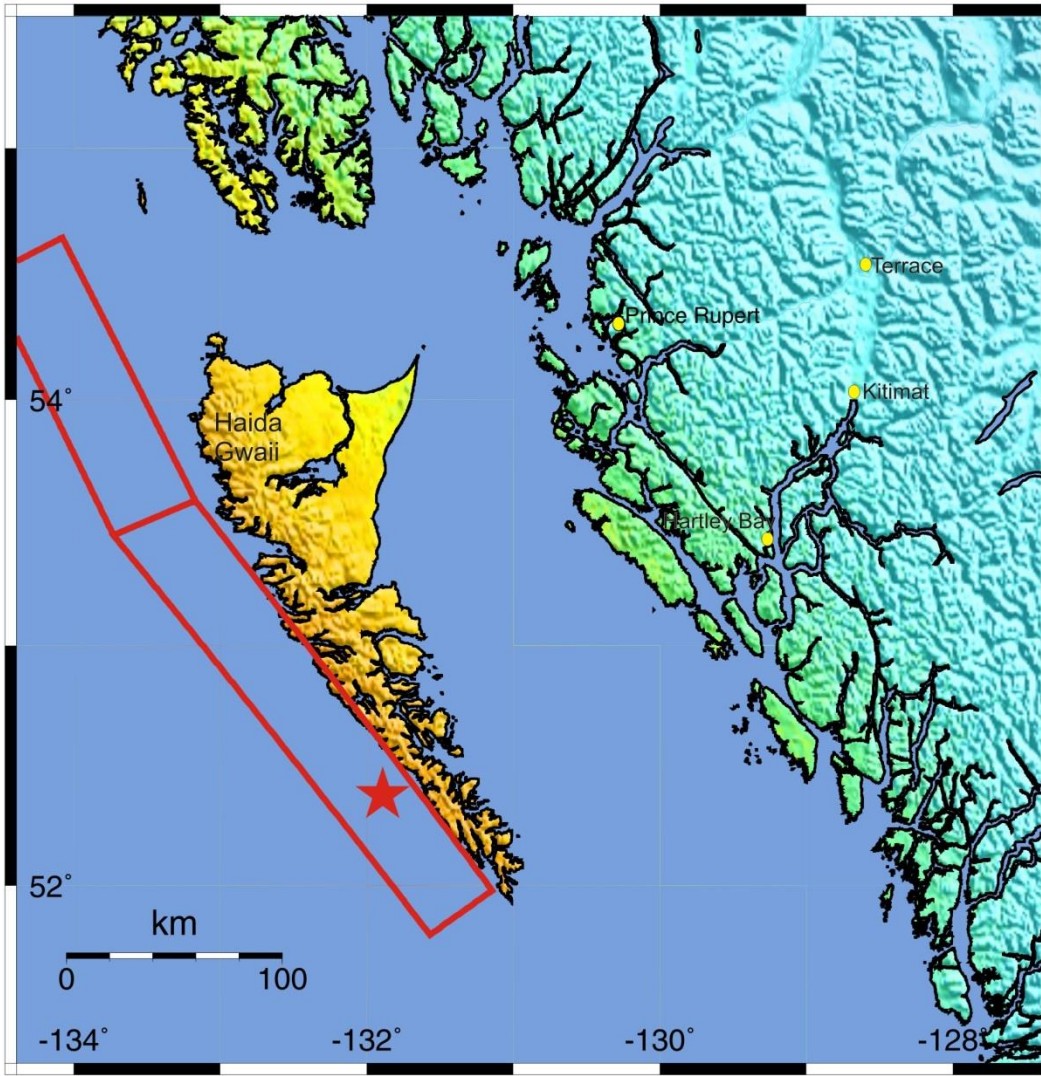


Figure 6 - Deaggregation of the 2005 NBCC for a central point in the BCNC (53.5N, 129.0W). Number in parenthesis is period in seconds.

-- Earthquake Planning Scenario --
 ShakeMap for Haida_Gwaii_Thrust Scenario

Scenario Date: SEP 11 2013 09:50:41 AM M 8.0 N52.38 W131.89 Depth: 20.0km

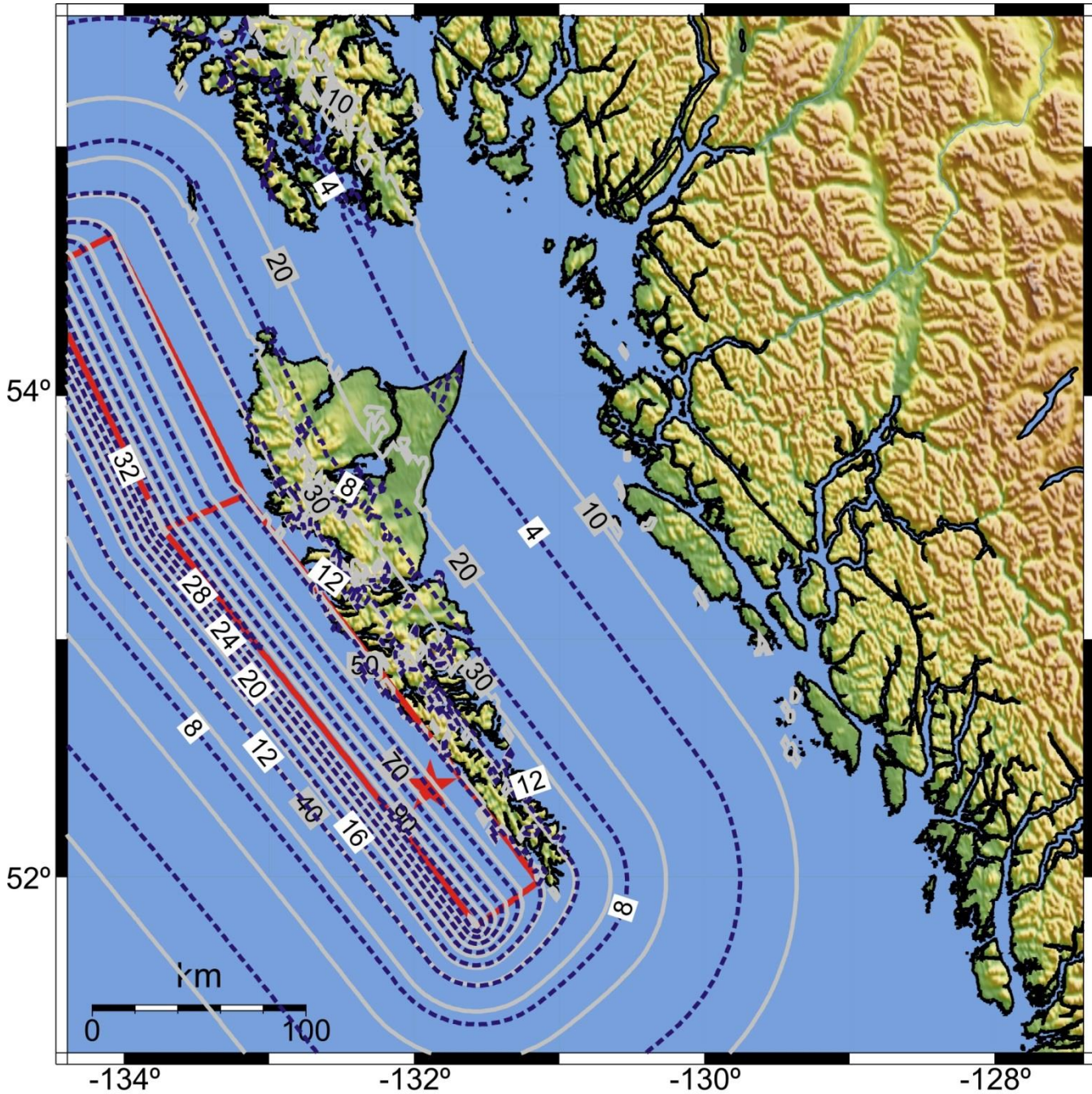


PLANNING SCENARIO ONLY -- Map Version 5 Processed Wed Dec 23, 2015 10:45:47 AM PST

PERCEIVED SHAKING	Not felt	Weak	Light	Moderate	Strong	Very strong	Severe	Violent	Extreme
POTENTIAL DAMAGE	none	none	none	Very light	Light	Moderate	Mod./Heavy	Heavy	Very Heavy
PEAK ACC.(%g)	<0.05	0.3	2.8	6.2	12	22	40	75	>139
PEAK VEL.(cm/s)	<0.02	0.1	1.4	4.7	9.6	20	41	86	>178
INSTRUMENTAL INTENSITY	I	II-III	IV	V	VI	VII	VIII	IX	X+

Scale based upon Worden et al. (2011)

Figure 7a – Estimated shaking intensities for Haida Gwaii Mw 8.0 thrust earthquake scenario. Red polygon represents rupture area, red star represents epicenter.

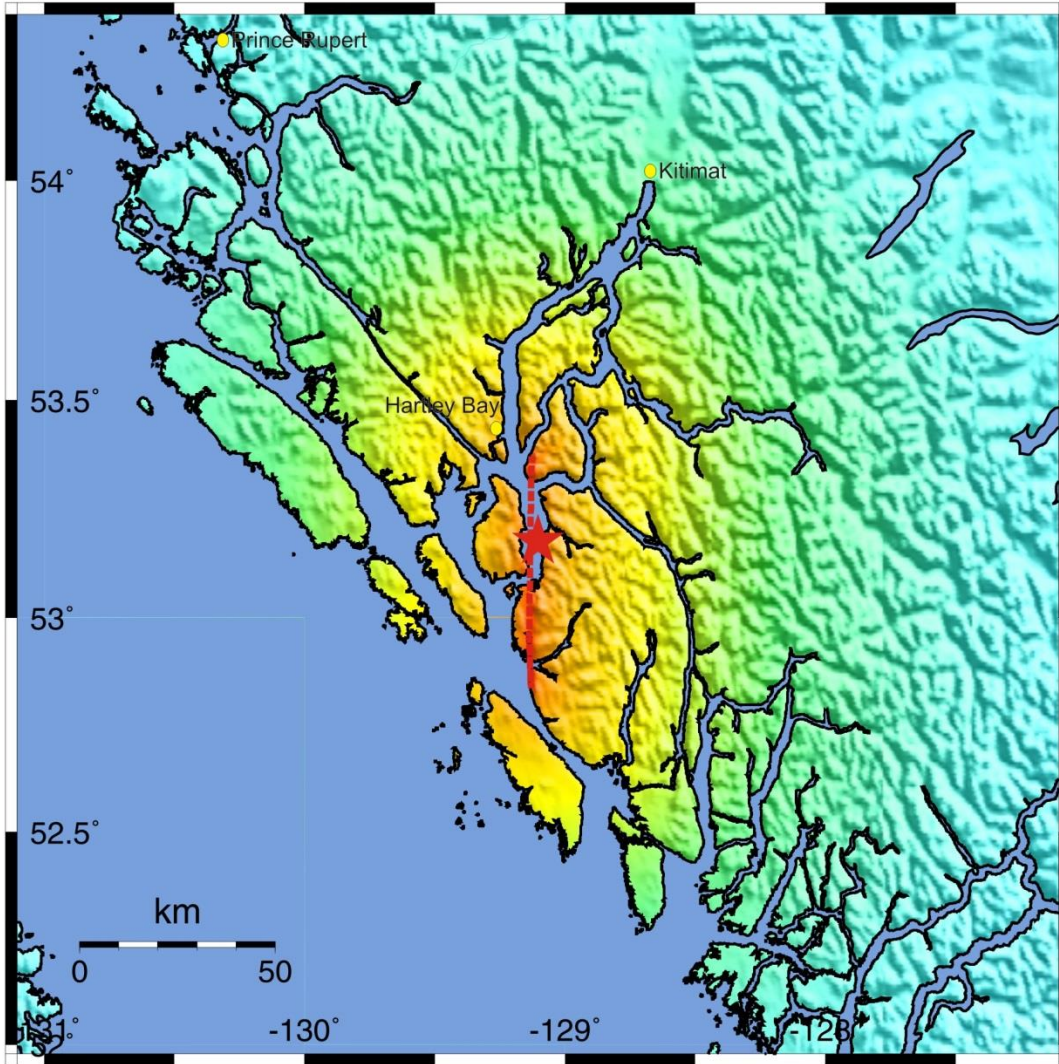


PLANNING SCENARIO ONLY -- Map Version 5 Processed Wed Dec 23, 2015 10:45:47 AM PST

Figure 7b - Sa(3.0) and Sa(1.0) for Haida Gwaii thrust earthquake scenario. Red polygon represents rupture area, red star represents epicenter, blue dashed lines and white labels are Sa(3.0) contours; grey contours and labels are Sa(1.0) in %g for this scenario.

-- Earthquake Planning Scenario --
 ShakeMap for Douglas_Channel Scenario

Scenario Date: SEP 11 2013 09:50:41 AM M 7.2 N53.18 W129.10 Depth: 33.0km



PLANNING SCENARIO ONLY -- Map Version 6 Processed Thu Sep 26, 2013 02:50:06 PM PDT

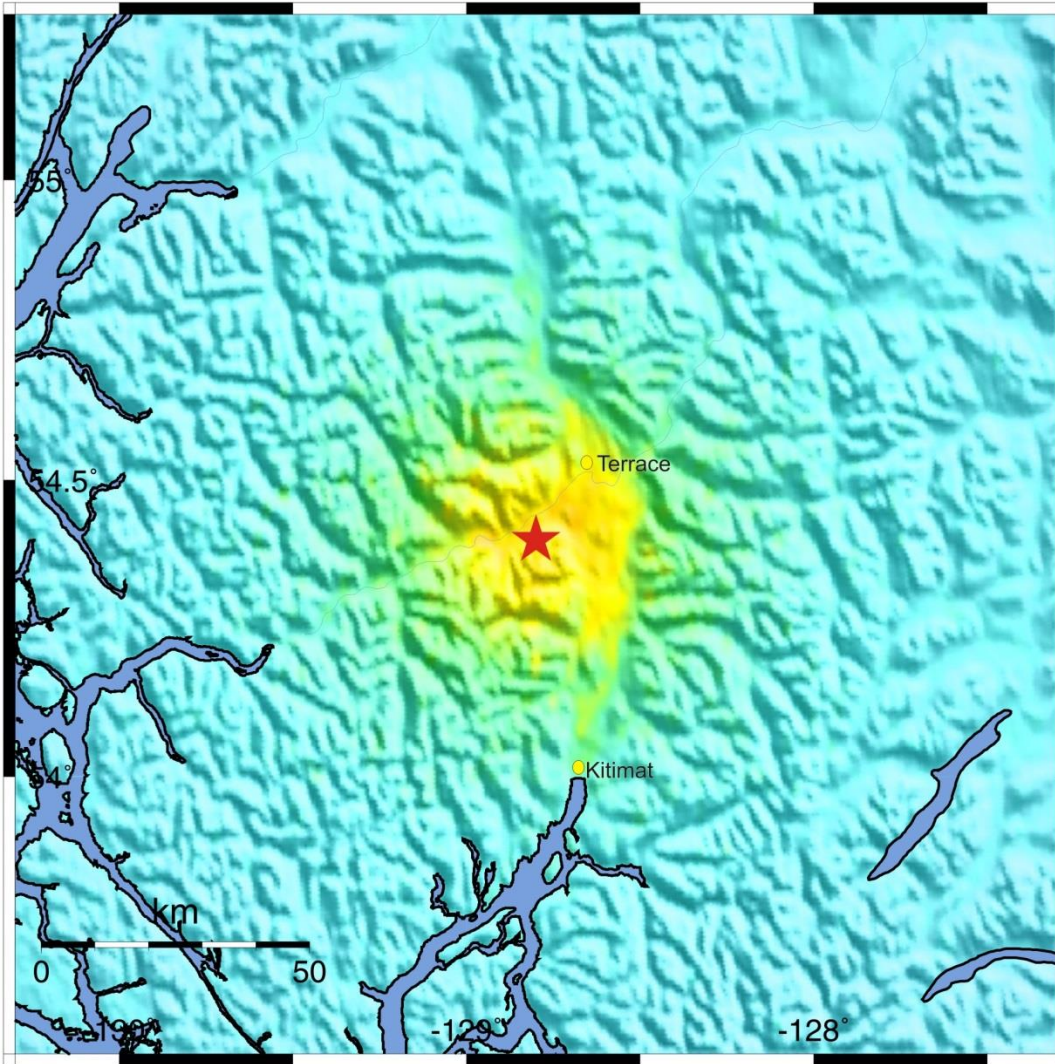
PERCEIVED SHAKING	Not felt	Weak	Light	Moderate	Strong	Very strong	Severe	Violent	Extreme
POTENTIAL DAMAGE	none	none	none	Very light	Light	Moderate	Mod./Heavy	Heavy	Very Heavy
PEAK ACC.(%g)	<0.05	0.3	2.8	6.2	12	22	40	75	>139
PEAK VEL.(cm/s)	<0.02	0.1	1.4	4.7	9.6	20	41	86	>178
INSTRUMENTAL INTENSITY	I	II-III	IV	V	VI	VII	VIII	IX	X+

Scale based upon Worden et al. (2011)

Figure 7c – Estimated shaking intensities for Douglas Channel fault earthquake scenario. Red dashed line represents fault rupture, red star represents epicenter.

-- Earthquake Planning Scenario --
 ShakeMap for Terrace Scenario

Scenario Date: SEP 11 2013 09:50:41 AM M 6.3 N54.40 W128.80 Depth: 10.0km



PLANNING SCENARIO ONLY -- Map Version 2 Processed Thu Sep 26, 2013 03:32:01 PM PDT

PERCEIVED SHAKING	Not felt	Weak	Light	Moderate	Strong	Very strong	Severe	Violent	Extreme
POTENTIAL DAMAGE	none	none	none	Very light	Light	Moderate	Mod./Heavy	Heavy	Very Heavy
PEAK ACC.(%g)	<0.05	0.3	2.8	6.2	12	22	40	75	>139
PEAK VEL.(cm/s)	<0.02	0.1	1.4	4.7	9.6	20	41	86	>178
INSTRUMENTAL INTENSITY	I	II-III	IV	V	VI	VII	VIII	IX	X+

Scale based upon Worden et al. (2011)

Figure 7d – Estimated shaking intensities for Terrace earthquake scenario. Red star represents epicenter.

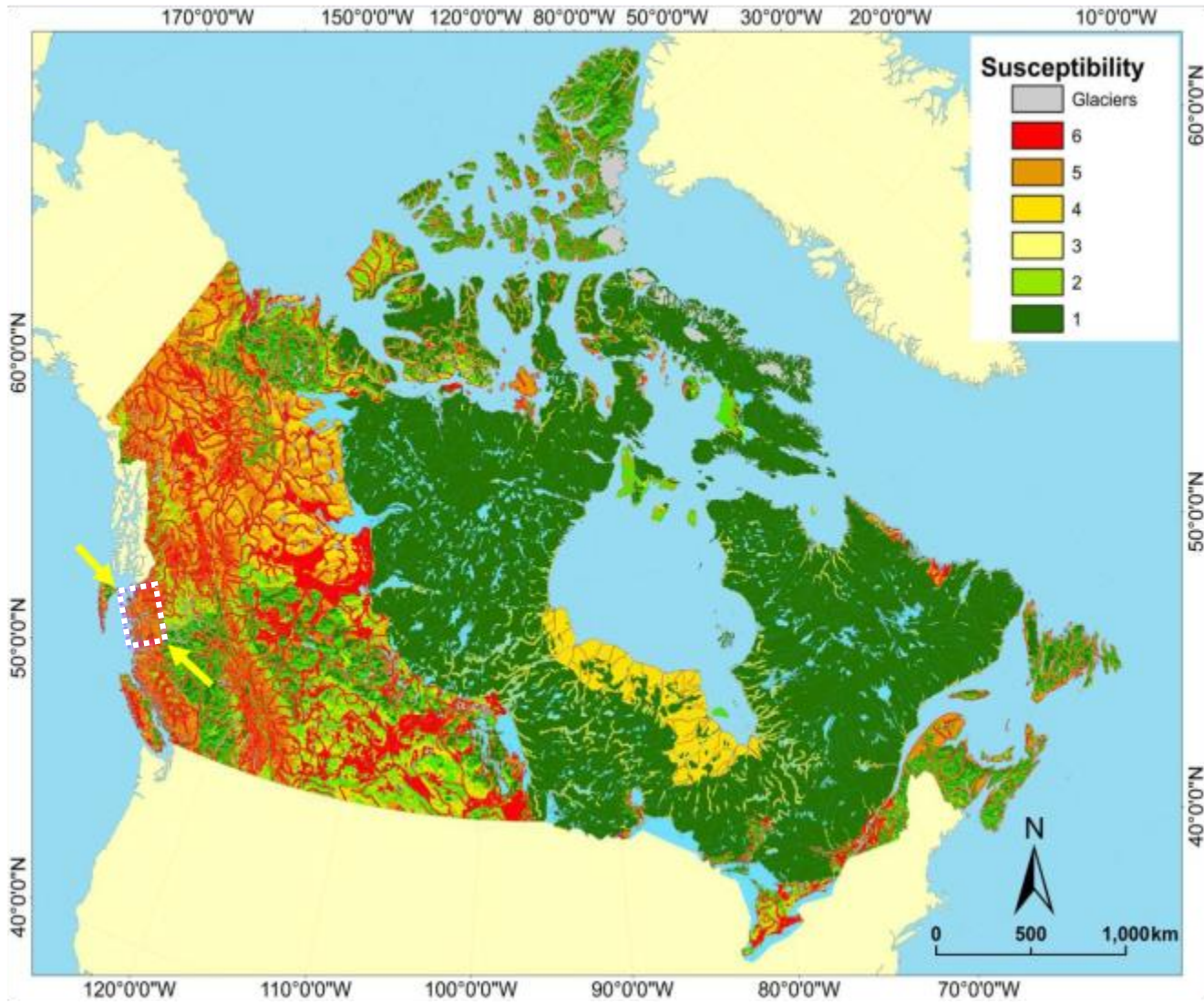


Figure 8 - Landslide susceptibility map of Canada. Yellow arrows and purple/white dashed outline is the location of the BCNC (after Bobrowsky and Dominguez, 2012).

Tables

Site ID	Location	Latitude	Longitude	Start Date
Seismograph stations prior to 2014				
BBB	Bella Bella	52.185	-128.113	1986-12-05
BNAB	Bonilla	53.493	-130.638	1999-04-16
BNB	Barry Inlet	52.576	-131.752	1985-09-06
CRAG	Craig, AK	55.470	-133.120	2004-12-10
DIB	Dawson Inlet	53.202	-132.477	2004-03-15
FSB	Fort St. James	54.477	-124.328	1979-04-30
HOLB	Holberg	50.641	-128.132	1994-09-01
LIB	Langara Island	54.256	-133.058	1984-09-12
MASB	Masset	54.015	-132.023	1999-04-15
MOBC	Moresby	53.144	-131.966	1996-02-26
NDB	Naden	53.955	-132.942	1987-09-15
PHC	Port Hardy	50.707	-127.433	1963-03-17
RUBB	Prince Rupert	54.326	-130.252	2001-07-18
UBRB	Upper Baezaeko River	52.892	-124.083	2007-10-16
VIB	Van Inlet	53.252	-132.541	1985-09-06
Seismic stations added/upgraded in 2014				
BNAB	Bonilla Island	53.492	-130.637	2014-03-25
BNKB	Banks Island	53.3318	-129.9017	2014-08-20
BUTB	near Butedale	53.063	-128.4633	2014-08-21
GRNB	near Grenville Channel	53.8468	-129.9575	2014-08-24
HWKB	Hawkesbury Island	53.5984	-129.1544	2014-08-21
KITB	Kitimat	54.078	-128.637	2014-03-20
GPS stations prior to September 2014				
BCPR	Pr. Rupert	54.28	-130.43	2004-11-04
BCTE	Terrace	54.51	-128.63	1996-06-21
BCSS	Sandspit	53.25	-131.81	2005-06-15
GPS stations added/upgraded in 2014				
BCDI	Bella Bella (updated)	52.16	-128.11	2015-03-27
BLBC	Bella Coola (updated)	52.38	-126.59	2015-03-19
BNAB	Bonilla Island (updated)	53.492	-130.637	2014-03-25
BNKB	Banks Island	53.3318	-129.9017	2014-08-20
BUTB	near Butedale	53.063	-128.4633	2014-08-21
GRNB	near Grenville Channel	53.8468	-129.9575	2014-08-24
HWKB	Hawkesbury Island	53.5984	-129.1544	2014-08-21
KTMT	Kitimat	54.098575	-128.61925	2015-09-25

Table 1 – Seismic and GPS stations in BC's north coast (see figures 3&4).

Probability of exceedance in 50 years	2%	5%	10%	40%
Sa(0.2)	0.364-0.388	0.238-0.262	0.161-0.189	0.061-0.091
Sa(0.5)	0.230-0.257	0.149-0.177	0.101-0.131	0.042-0.066
Sa(1.0)	0.123-0.163	0.082-0.111	0.057-0.082	0.0260.040
Sa(2.0)	0.07-0.093	0.047-0.064	0.034-0.047	0.0160.024
PGA	0.172-0.184	0.117-0.129	0.083-0.097	0.0340.050

Table 2 - Probabilistic seismic hazard for BCNC based on 2010 NBCC.

Site Class	Values of F_a					Values of F_v				
	$S_a(0.2) \leq 0.25$	$S_a(0.2) = 0.50$	$S_a(0.2) = 0.75$	$S_a(0.2) = 1.00$	$S_a(0.2) \geq 1.25$	$S_a(1.0) \leq 0.1$	$S_a(1.0) = 0.2$	$S_a(1.0) = 0.3$	$S_a(1.0) = 0.4$	$S_a(1.0) \geq 0.5$
A	0.7	0.7	0.8	0.8	0.8	0.5	0.5	0.5	0.6	0.6
B	0.8	0.8	0.9	1.0	1.0	0.6	0.7	0.7	0.8	0.8
C	1.0	1.0	1.0	1.0	1.0	1.0	1.0	1.0	1.0	1.0
D	1.3	1.2	1.1	1.1	1.0	1.4	1.3	1.2	1.1	1.1
E	2.1	1.4	1.1	0.9	0.9	2.1	2.0	1.9	1.7	1.7
F	(1)	(1)	(1)	(1)	(1)	(1)	(1)	(1)	(1)	(1)

(1) To determine F_a and F_v for site Class F, site specific geotechnical investigations and dynamic site response analyses shall be performed.

Table 3 - Values of soil modification factors (F_a and F_v) as a function of site class and $S_a(0.2)$ and $S_a(1.0)$ (from Halchuck, 2007).

References

- AMEC (2010). *Preliminary Geotechnical Report Proposed Kitimat Terminal Enbridge Northern Gateway Project Kitimat, British Columbia*. Prepared for: Northern Gateway Pipelines Inc.
- Adams, J., & Halchuck, A. (2007). A Review of NBCC 2005 Seismic Hazard Results for Canada - The Interface to the Ground and Prognosis for Urban Risk Mitigation. *OttawaGeo2007: Proceedings, Canadian Geotechnical Conference Annual Meeting*, 837-846.
- Adams, J., & Halchuck, S. (2003). *Fourth Generation seismic hazard maps of Canada: Values for over 650 Canadian localities intended for the 2005 National Building Code of Canada*. Geological Survey of Canada, Open File 4459, p. 155. doi:10.4095/21422.
- Allen, T., & Wald, D. (2009). On the Use of High-Resolution Topographic Data as a Proxy for Seismic Site Conditions (VS30). *Bulletin of the Seismological Society of America*, 99(2A), 935-943.
- Altamimi, Z., Sillard, P., & Boucher, C. (2002). ITRF2000: A New Release of the International Terrestrial Reference Frame for Earth Science Applications. *Journal of Geophysical Research:Solid Earth*, 107(B10), ETG-2. doi:10.1029/2001JB000561
- Arias, A. (1970). *A measure of earthquake intensity, in Seismic Design for Nuclear Power Plants*. (R. J. Hansen, Ed.) Cambridge, MA: The MIT Press.
- Atwater, B.F., Nelson, A.R., Clague, J.J., Carver, G.A., Yamaguchi, D.K., Bobrowsky, P.T., Bourgeois, J., Darienzo, M.E., Grant, W.C., Hemphill-Haley, E. and Kelsey, H.M. (1995). Summary of Coastal Geologic Evidence for Past Great Earthquakes at the Cascadia Subduction Zone. *Earthquake Spectra*, 11(1), 1-18.
- BC Ministry of Environment. *Ecology*. Retrieved 10 2013, from <http://www.env.gov.bc.ca/ecology/ecoregions/humidtemp.html>.
- Benjamin, J. R. (1988). *A Criterion for Determining Exceedances of the Operating Basis Earthquake*, EPRI Report NP-5930. Electric Power Research Institute, Palo Alto.
- Bird, A., & Lamontagne, M. (2015). Impacts of the October 2012 magnitude 7.8 earthquake near Haida Gwaii, Canada, *Bulletin of the Seismological Society of America*, 105(2B), 1178-1192. doi:10.1785/0120140167
- Bobrowsky, P., & Dominguez, M. (2012). *Landslide susceptibility map of Canada*. Geological Survey of Canada, Open File 7228, 1 sheet. doi:10.4095/291902
- Booth, D. B., Goetz Troost, K., Clague, J. J., & Waitt, R. B. (2003). The Cordilleran ice sheet. *Development in Quaternary Science*, 1, 17-43. doi:10.1016/S1571-0866(03)01002-9
- Bornhold, B.D. (1983). Sedimentation in Douglas Channel and Kitimat Arm. *Canadian Technical Report of Hydrology and Ocean Sciences*, 18, 88-114.
- Bostwick, T. (1984). *A Re-examination of the August 22, 1949 Queen Charlotte Earthquake* (M.Sc. dissertation), University of British Columbia, Vancouver, BC.
- Brooks, G. R. (2013). A massive sensitive clay landslide, Quyon Valley, southwestern Quebec, Canada, and evidence for a paleoearthquake triggering mechanism, *Quaternary Research*. 80(3), 425-434.
- Campbell, D., & Skermer, N. (1975). *Report to B. C. Water Resources Service on Investigation of Sea Wave at Kitimat*. BC Golder Associates, Vancouver.

- Cassidy, J.F., Balfour, N., Hickson, C., Kao, H., White, R., Caplan-Auerbach, J., Mazzotti, S., Rogers, G.C., Al-Khoubbi, I., Bird, A.L. and Esteban, L. (2011). The 2007 Nazko, British Columbia, Earthquake Sequence: Injection of Magma Deep in the Crust beneath the Anahim Volcanic Belt. *Bulletin of the Seismological Society of America*, 101(4), 1732-1741. doi:10.1785/0120100013
- Cassidy, J., Rogers, G., Lamontagne, M., Halchuk, S., & Adams, J. (2010). Canada's Earthquakes: 'The Good, the Bad, and the Ugly'. *Geoscience Canada*, 37(1). doi:10.12789/gsc.v37i1.15300
- Chardon, D., Andronicos, C. L., & Hollister, L. S. (1999). Large-scale transpressive shear zone patterns and displacements within magmatic arcs: The Coast Plutonic Complex, British Columbia, *Tectonics* 18(2), 278-292.
- Chiou, B. S., & Youngs, R. R. (2008). An NGA model for the average horizontal component of peak ground motion and response spectra. *Earthquake Spectra*, 24(S1), 173-215.
- Clague, J. (1984). Deglaciation of Prince Rupert - Kitimat area, British Columbia. *Canadian Journal of Earth Sciences*, 22(2), 256-265.
- Conway, K., Barrie, J., & Thomson, R. (2012). Submarine slope failures and tsunami hazard in coastal British Columbia: Douglas Channel and Kitimat Arm. *Geological Survey of Canada, Current Research 2012-10*, p. 13. doi:10.4095/291732
- Cua, G., Wald, D., Allen, T., Garcia, D., Worden, C., Lin, K., & Marano, K. (2010). "Best Practices" for using macroseismic intensity and ground-motion intensity conversion equations for hazard and loss models in GEM1, p. 4. GEM Technical Report 2010-4, GEM Foundation, Pavia, Italy. (www.globalquakemodel.org)
- Cubrinovski, M., Bray, J. D., Taylor, M., Giorgini, S., Bradley, B., Wotherspoon, L., & Zupan, J. (2011). Soil liquefaction effects in the central business district during the February 2011 Christchurch earthquake. *Seismological Research Letters*, 82(6), 893-904, doi: 10.1785/gssrl.82.6.893.
- Dai, F. C., Xu, C., Yao, X., Xu, L., Tu, X. B., & Gong, Q. M. Spatial distribution of landslides triggered by the 2008 Ms 8.0 Wenchuan earthquake, China. *Journal of Asian Earth Sciences*, 40(4), 883-895.
- Dengler, L. A., and J. W. Dewey (1998). An intensity survey of households affected by the Northridge, California, earthquake of 17 January, 1994, *Bulletin of the Seismological Society of America*, 88, 441-462.
- Dolmage, V. (1956). Geology of Kitimat Area, British Columbia (103 IELI2). *Geological Survey of Canada Memoir*, 329.
- Dominguez, Cuesta, M., & Bobrowsky, P. T. (2011). Proposed landslide susceptibility map of Canada based on GIS. In *Landslide Science and Practice* (pp. 375-382). Springer Berlin Heidelberg.
- Environment Canada. *Historical Climate Data*. Retrieved 11 2013, from http://climate.weather.gc.ca/index_e.html#access
- Finn, W. L., & Wightman, A. (2003). Ground motion amplification factors for the proposed 2005 edition of the National Building Code of Canada. *Canadian Journal of Civil Engineering*, 30(2), 272-278. doi: 10.1139/L02-081
- Fry, B., Benites, R., & Kaiser, A. (2011). The Character of Accelerations in the Mw 6.2 Christchurch Earthquake. *Seismological Research Letters*, 82(6), 846-852. doi: 10.1785/gssrl.82.6.846
- Geertsema, M., Clague, J. J., Schwab, J. W., & Evans, S. G. (2006). An overview of recent large catastrophic landslides in northern British Columbia, Canada. *Engineering Geology*, 83(1), 20-143.

- Gehrels, G., Rusmore, M., Woodsworth, G., Crawford, M., Andronicos, C., Hollister, L., Patchett, J., Ducea, M., Butler, R., Klepeis, K. and Davidson, C. (2009). U-Th-Pb geochronology of the Coast Mountains batholith in north-coastal British Columbia: Constraints on age and tectonic evolution. *Geological Society of America Bulletin*, 121(9-10), 1341-1361.
- Godt, J., Sener, B., Verdin, K., Wald, D., Earle, P., Harp, E., & Jibson, R. (2008, November). Rapid assessment of earthquake-induced landsliding. In *Proceedings of the First World Landslide Forum, United Nations University, Tokyo* (Vol. 4, pp. 3166-1).
- Goldfinger, C., Nelson, C. H., Morey, A. E., Johnson, J. E., Patton, J. R., Karabanov, E., Gutiérrez-Pastor, J., Eriksson, A. T., Gràcia, E., Dunhill, G., Enkin, R. J., Dallimore, A., and Vallier, T. (2012). Turbidite event history—Methods and implications for Holocene paleoseismicity of the Cascadia subduction zone (pp. 1-159). US Department of the Interior, US Geological Survey.
- Hanks, T. C., & Bakun, W. H. (2002). M-logA observations for recent large earthquakes. *Bulletin of the Seismological Society of America*, 98(1), 490-494.
- Hansen, A., & Franks, C. (1991). Characterisation and Mapping of Earthquake Triggered Landslides for Seismic Zonation. In *Proceedings of the Fourth International Conference on Seismic Zonation*, Stanford, California (Vol. 1, pp. 149-195).
- Hippchen, S. (2011). *Slip Partitioning, Crustal Tectonics and Deformation of the Queen Charlotte Margin and Northern Vancouver Island* (PhD. Dissertation), University of Victoria, School of Earth and Ocean Sciences, Victoria, BC, Canada.
- Hyndman, R. D. (2013). Downdip landward limit of Cascadia great earthquake rupture. *Journal of Geophysical Research: Solid Earth*, 118(10), 5530-5549. doi:10.1002/jgrb.50390
- Hyndman, R., & Hamilton, T. (1993). Queen Charlotte area Cenozoic tectonics and volcanism and their association with relative plate motions along the northeastern Pacific Margin. *Journal of Geophysical Research: Solid Earth*, 98(B8), 14257-14277.
- Hyndman, R., Rogers, G., Dragert, H., Wang, K., Clague, J., Adams, J., & Bobrowsky, P. (1996). Giant Earthquakes beneath Canada's West Coast. *Geoscience Canada*, 23(2), 63-72.
- Hunter, J.A. and Crow, H.L. (ed.), 2012. *Shear Wave Velocity Measurement Guidelines for Canadian Seismic Site Characterization in Soil and Rock*. Geological Survey of Canada, Open File 7078, p. 227. doi:10.4095/291753.
- Jakob, M., Holm, K., Lange, O., & Schwab, J. W. (2006). Hydrometeorological thresholds for landslide initiation. *Landslides*, 3(3), 228-238.
- James, T., Rogers, G., Cassidy, J., Dragert, H., Hyndman, R., Leonard, L., Nykolaishen, L., Riedel, M., Schmidt, M. and Wang, K. (2013). Field Studies Target Haida Gwaii Earthquake. *Eos, Transactions American Geophysical Union*, 94(22), 197-198.
- James, T. S., Cassidy, J. F., Rogers, G. C., & Haeussler, P. J. (2015). Introduction to the Special Issue on the 2012 Haida Gwaii and 2013 Craig Earthquakes at the Pacific–North America Plate Boundary (British Columbia and Alaska). *Bulletin of the Seismological Society of America*.
- Jibson, R. W., Harp, E. L., Schulz, W., & Keefer, D. K. (2004). Landslides triggered by the 2002 Denali Fault, Alaska, Earthquake and the Inferred Nature of the Strong Shaking. *Earthquake Spectra*, 20(3), 669-691.

- Kao, H., Shan, S.J., Bent, A., Woodgold, C., Rogers, G., Cassidy, J. F., & Ristau, J. (2012). Regional Centroid-Moment-Tensor Analysis for Earthquakes in Canada and Adjacent Regions: An Update. *Seismological Research Letters*, 83(3), 505-515. doi:10.1785/gssrl.83.3.505
- Kayen, R., Thompson, E., Minasian, D., Collins, B., Moss, E. R., Sitar, N., & Carver, G. (2004). 'Geotechnical Observations of the November 3, 2002 M7.9 Denali Fault Earthquake. In *Proceedings of the Fifth International Conference on Case Histories in Geotechnical Engineering*, New York.
- Keefer, D. (1984). Landslides Caused by Earthquakes. *Geological Society of America Bulletin*, 95(4), 406–421.
- Keefer, D. K. (2002). Investigating Landslides Caused by Earthquakes - A Historical Review. *Surveys in Geophysics*, 23(6), 473-510.
- Lamontagne, M., Halchuk, S., Cassidy, J., & Rogers, G. (2008). Significant Canadian Earthquakes of the period 1600-2006. *Seimological Research Letters*, 79(2), 211-223.
- Langston, Charles A. (1987). Depth of Faulting During the 1968 Meckering, Australia Sequence Determined From Waveform Analysis of Local Seismograms. *Journal of Geophysical Research*, 92(11), 11561-11574.
- Lee, C.T., Huang, C.C., Lee, J.F., Pan, K.L., Lin, M. L., & Dong, J. J. (2008). Statistical approach to earthquake-induced landslide susceptibility. *Engineering Geology*, 100(1), 43-58.
- Leonard, L. J. & Bednarski, J. M. (2015). The Preservation Potential of Coastal Coseismic and Tsunami Evidence Observed Following the 2012 Mw7.8 Haida Gwaii Thrust Earthquake. *Bulletin of the Seismological Society of America*, 105(2b). doi:10.1785/0120140193
- Leonard, L. J., Hyndman, R. D., Mazzotti, S., Nykolaishen, L., Schmidt, M., & Hippchen, S. (2007). Current Deformation in the Northern Cordillera Inferred from GPS Measurements. *Journal of Geophysical Research: Solid Earth*, 112(B11). doi:10.1029/2007JB005061
- Leonard, L. J., Rogers, G. C., & Mazzotti, S. (2014). Tsunami Hazard Assessment of Canada. *Natural Hazards*, 70(1), 237-274.
- Leonard, M. (2010). Earthquake fault scaling: Self-consistent relating of rupture length, width, average displacement, and moment release. *Bulletin of the Seismological Society of America*, 100(5A), 1971-1988.
- Mathews, W. (1979). Landslides of Central Vancouver Island and the 1946 Earthquake. *Bulletin of the Seismological Society of America*, 69(2), 445-450.
- Mazzotti, S., Dragert, H., Henton, J., Schmidt, M., Hyndman, R., James, T., Lu, Y. and Craymer, M. (2003a). Current Tectonics of Northern Cascadia from a Decade of GPS Measurements. *Journal of Geophysical Research*, 108(B12). doi:10.1029/2003JB002653
- Mazzotti, S., Hyndman, R., Fluck, P., Smith, A., & Schmidt, M. (2003b). Distribution of the Pacific/North American motion in the Queen Charlotte Islands-S. Alaska plateboundary zone. *Geophysical Research Letters*, 30(14), 1762.
- Miles, S., & Keefer, D. (2009). Evaluation of CAMEL—Comprehensive areal model of earthquake-induced landslides. *Engineering Geology*, 104(1), 1-15.
- Milne, W., Rogers, G., Riddihough, R., McMechan, G., & Hyndman, R. (1978). Seismicity of Western Canada. *Canadian Journal of Earth Science*, 15(7), 1170-1193.

- Mulder, T.A. (2005). Seismicity Catalogue: Western Canada. *SSA 2005 Meeting*, 27-29 April, Lake Tahoe, Nevada, USA, Poster L8.
- Murty, T. (1979). Submarine Slide-Generated Water Waves in Kitimat Inlet, British Columbia. *Journal of Geophysical Research: Oceans*, *81(C12)*, 7777-7779.
- Murty, T., & Brown, R. (1979). *The Submarine Slide of 27 April, 1975 in Kitimat Inlet and the Water Waves That Accompanied the Slide*. Department of Fisheries and the Environment, Institute of Ocean Sciences, Sidney, BC.
- Monger, J. W. H., Price, R. A., & Tempelman-Kluit, D. J. (1982). Tectonic accretion and the origin of the two major metamorphic and plutonic belts in the Canadian Cordillera. *Geology*, *10(2)*, 70-75.
- Nelson, J.L., Diakow, J.B., Mahoney, J.B., van Staal, C., Pecha, M., Angen, J., Gehrels, G. and Lau, T. (2012). *North Coast Project: Tectonics and Metallogeny of the Alexander Terrane, and Cretaceous Sinistral Shearing of the Western Coast Belt*. *British Columbia Ministry of Energy and Mines Paper, 1*, 157-180.
- O'Hara, T. F., & Jacobson, J. P. (1991). *Standardization of the cumulative absolute velocity* (No. EPRI-TR-100082). Electric Power Research Inst., Palo Alto, CA (United States); Yankee Atomic Electric Co., Bolton, MA (United States).
- Olson, S.M., Green, R.A., Lasley, S., Martin, N., Cox, B.R., Rathje, E., Bachhuber, J. and French, J. (2011). Documenting Liquefaction and Lateral Spreading Triggered by the 12 January 2010 Haiti Earthquake. *Earthquake Spectra*, *27(S1)*, 93-116.
- Page, R. A., Biswas, N. N., Lahr, J. C., & Pulpan, H. (1991). Seismicity of continental Alaska. In D. B. Slemmons, E. R. Engdahl, M. D. Zoback, & D. D. Blackwell (Eds.), *Neotectonics of North America*: Boulder, Colorado, USA: Geological Society of America, Decade Map Volume 1.
- Reasenber, P. A., Hanks, T. C., & Bakun, W. H. (2003). An empirical model for earthquake probabilities in the San Francisco Bay Region, California, 2002-2031. *Bulletin of the Seismological Society of America*, *93(1)*, 1-13.
- Ristau, J., Rogers, G. C., & Cassidy, J. F. (2007). Stress in Western Canada from Regional Moment Tensor Analysis. *Canadian Journal of Earth Science*, *44*, 127-148. doi:10.1139/E06-057
- Rodríguez, C. B. (1999). Earthquake-induced Landslides: 1980- 1997. *Soil Dynamics and Earthquake Engineering*, *18(5)*, 325-346.
- Rogers, G. (1986). Seismic gaps along the Queen Charlotte Fault: *Earthquake Prediction Research*. *4(1-2)*, 1-11.
- Rogers, G. C. (1976). The Terrace earthquake of 5 November 1973. *Canadian Journal of Earth Sciences*, *13(4)*, 495-499.
- Rogers, G. C. (1980). A documentation of soil failure during the British Columbia earthquake of 23 June, 1946. *Canadian Geotechnical Journal*, *17(1)*, 122-127.
- Rohr, K. M. M., & Dietrich, J.R. (1992). Strike-slip tectonics and development of the Tertiary Queen Charlotte Basin, offshore western Canada: Evidence from seismic reflection data. *Basin Research*, *41(1)*, 1-19, doi: 10.1111/j.1365-2117.1992.tb00039.x.
- Satake, K., Shimazaki, K., Tsuji, Y., & Ueda, K. (1996). Time and size of a giant earthquake in Cascadia inferred from Japanese tsunami records of January 1700. *Nature*, *379(6562)*, 246-249. doi:10.1038/379246a0
- Saunders, W., & Berryman, K. (2012). *Just add water: when should liquefaction be considered in land use planning?* GNS Science Miscellaneous Series 47.

- Schwab, J. W. (2011). *Hillslope and Fluvial Processes along the proposed pipeline corridor, Burns Lake to Kitimat, West Central British Columbia*. Smithers, BC: Buckley Valley Research Center for Natural Resource Research and Management, Smithers, BC.
- Seed, B., & Lee, K. (1966). Liquefaction of Saturated Sands During Cyclic Loading. *Journal of Soil Mechanics & Foundations Division*, 92(6), 105-134.
- Shaw, B. E. (2009). Constant Stress Drop from Small to Great Earthquakes in Magnitude-Area Scaling. *Bulletin of the Seismological Society of America*, 99(2A), 871-875.
- Shearer, P.M. & Orcutt, J.A. (1987). Surface and near-surface effects on seismic waves - theory and borehole seismometer results. *Bulletin of the Seismological Society of America*, 77(4), 1168-1196.
- Skvortsov, A., & Bornhold, B. (2007). Numerical simulation of the landslide-generated tsunami in Kitimat Arm, British Columbia, Canada, 27 April 1975. *Journal of Geophysical Research: Earth Surface*, 112(F2). doi:10.1029/2006JF000499
- Slawson, W., & Savage, J. (1979). Geodetic Deformation Associated with the 1946 Vancouver Island, Canada Earthquake. *Bulletin of the Seismological Society of America*, 69(5), 1487-1496.
- Strasser, F. O., Arango, M. C., & Bommer, J. J. (2010). Scaling of the source dimensions of interface and intraslab subduction-zone earthquakes with moment magnitude, *Seismological Research Letters*, 81(6), 941-950.
- U.S. Geological Survey (2008). Magnitude 7.9 — Eastern Sichuan, China, 2008 May 12 06:28:01 UTC. Retrieved from <http://earthquake.usgs.gov/earthquakes/eqinthenews/2008/us2008ryan/us2008ryan.php>.
- Wald, D., & Allen, T. (2007). Topographic Slopes as a proxy for seismic site conditions and amplification. *Bulletin of the Seismological Society of America*, 97(5), 1379-1395.
- Wald, D., Quitoriano, V., Heaton, T., & Kanamori, H. (1999a). Relationships between peak ground acceleration, peak ground velocity and Modified Mercalli intensity in California. *Earthquake Spectra*, 15(3), 557-564.
- Wald, D. J., Quitoriano, V., Heaton, T. H., Kanamori, H., Scrivner, C. W., & Worden, B. C. (1999b). TriNet "ShakeMaps": Rapid generation of peak ground-motion and intensity maps for earthquakes in southern California, *Earthquake Spectra* 15(3), 537-556.
- Walsh, T. J., Combellick, R. A., & Black, G. L. (1995) *Liquefaction features from a subduction zone earthquake: preserved examples from the 1964 Alaska earthquake* (No. 32). Washington State Department of Natural Resources, Division of Geology and Earth Resources.
- Wang, C. Y., & Manga, M. (2010). *Earthquakes and water* (Vol. 114). Springer. doi:10.1007/978-3-642-00810-8_2
- Wang, C., Wong, A., Dreger, D. S., & Manga, M. (2006). Liquefaction limit during earthquakes and underground explosions—Implications on ground-motion attenuation. *Bulletin of the Seismological Society of America*, 96(1), 355–363.
- Wang, C.Y., Dreger, D. S., Wang, C.H., Mayeri, D., & Berryman, J. G. (2003). Field relations among coseismic ground motion, water level change and liquefaction for the 1999 Chi-Chi (Mw = 7.5) earthquake, Taiwan. *Geophysical Research Letters*, 30(17). doi:10.1029/2003GL017601
- Wells, D. L., & Coppersmith, K. J. (1994). New empirical relationships among magnitude, rupture length, rupture width, rupture area, and surface displacement. *Bulletin of the Seismological Society of America*, 84(4), 974-1002.

- Wong, A., & Wang, C. Y. (2007). Field relations between the spectral composition of ground motion and hydrological effects during the 1999 Chi-Chi (Taiwan) earthquake. *Journal of Geophysical Research: Solid Earth*, *112*(B10). doi:10.1029/2006JB004516
- Wood, H., & Neumann, F. (1931). Modified Mercalli Intensity Scale of 1931. *Bulletin of the Seismological Society of America*, *21*, 277-283.
- Worden, C., Gerstenberger, M., Rhoades, D., & Wald, D. (2012). Probabilistic Relationships between Ground-Motion Parameters and Modified Mercalli Intensity in California. *Bulletin of the Seismological Society of America*, *102*(1), 204-221.
- Zhao, J. X., Zhang, J., Asano, A., Ohno, Y., Oouchi, T., Takahashi, T., Ogawa, H., Irikura, K., Thio, H.K., Somerville, P.G. & Fukushima, Y. (2006). Attenuation relations of strong ground motion in Japan using site classification based on predominant period. *Bulletin of the Seismological Society of America*, *96*(3), 898-913.